The Value of Wind Profiler Data in U.S. Weather Forecasting

Stanley G. Benjamin
Barry E. Schwartz
Edward J. Szoke[1]
Steven E. Koch

NOAA Research – Forecast Systems Laboratory
Boulder, Colorado 80305

Manuscript plus online supplement
Accepted for publication in
Bulletin of the American Meteorological Society

25 March 2004

[1] In collaboration with the Cooperative Institute for Research in the Atmospheres (CIRA), Colorado State University, Ft. Collins, CO
Corresponding author: Stan Benjamin, stan.benjamin@noaa.gov, phone – 303-497-6387, fax – 303-497-7262, Mail – NOAA/FSL, 325 Broadway, R/E/FS1, Boulder, CO 80305 USA

Abstract

An assessment of the value of data from the NOAA Profiler Network (NPN) on weather forecasting is presented. A series of experiments was conducted using the Rapid Update Cycle (RUC) model/assimilation system in which various data sources were denied to assess the relative importance of the profiler data for short-range wind forecasts. Average verification statistics from a 13-day cold-season test period indicate that the profiler data have a positive impact on short-range (3-12 h) forecasts over the RUC domain containing the lower 48 United States, strongest at 3-h projection over a central U.S. subdomain that includes most of the profiler sites as well as downwind of the profiler observations over the eastern U.S. Overall, profiler data reduce wind forecast errors at all levels from 850-150 hPa, especially below 300 hPa where there are relatively few automated aircraft observations. At night when fewer commercial aircraft are flying, profiler data also contribute strongly to more accurate 3-h forecasts, including near-tropopause maximum wind levels. For the test period, the profiler data contributed up to 20-30% (at 700 hPa) of the overall reduction of 3-h wind forecast error by all data sources combined. Inclusion of wind profiler data also reduced 3-h errors for height, relative humidity and temperature by 5-15%, averaged over different vertical levels. Time series and statistics from large error events demonstrate that the impact of profiler data may be much larger in peak error situations.

Three data assimilation case studies from cold and warm seasons are presented that illustrate the value of the profiler observations for improving weather forecasts. The first case study indicates that inclusion of profiler data in the RUC model runs for the 3 May

1999 Oklahoma tornado outbreak improved model guidance of convective available potential energy (CAPE), 300 hPa wind, and precipitation in southwestern Oklahoma at the onset of the event. . In the second case study, inclusion of profiler data led to better RUC precipitation forecasts associated with a severe snow and ice storm that occurred over the central plains of the United States in February 2001. A third case study describes the effect of profiler data for a tornado event in Oklahoma on 8 May 2003. Summaries of National Weather Service (NWS) forecaster use of profiler data in daily operations, although subjective, support the results from these case studies and the statistical forecast model impact study in the broad sense that profiler data contribute significantly to improved short-range forecasts over the central U.S. where these observations currently exist.

1. Introduction

The National Oceanic and Atmospheric Administration (NOAA) Forecast Systems Laboratory (FSL) has operated a network of 404-MHz tropospheric wind profilers since 1992 (http://www.profiler.noaa.gov/jsp/aboutNpnProfilers.jsp, van de Kamp 1993, Weber et al. 1990). Most of these platforms operate over the central United States (U.S.), with the exception of a few profilers in Alaska and elsewhere (Fig. 1). The role of wind profiler data in forecaster decision-making is typified in the following two accounts regarding significant weather events:

> The NOAA Storm Prediction Center (SPC) in Norman, Oklahoma, located in the middle of the NOAA Profiler Network (NPN), has a high interest in monitoring evolving low-level and deep vertical wind shear conducive to severe thunderstorms. SPC forecasters frequently use the profiler data for issuing both Convective Outlooks as well as Watches, with the data often critical for determining the level of severity expected. A prime example occurred with the 3 May 1999 Oklahoma-Kansas tornado outbreak (Edwards et al. 2002). The forecasters on 3 May observed considerably stronger winds at the Tucumcari, New Mexico, profiler site than were forecasted by the models. Extrapolation of these winds to the afternoon threat area gave the forecasters confidence that tornadic storms with organized supercells would be the main mode of severe weather risk. Based on the likelihood of stronger vertical wind shear, the risk would be greater than previously suggested by numerical models. Armed with the profiler observations, SPC forecasters first increased the threat in the current-day convective outlook from slight to moderate risk, and then to high risk by

mid-afternoon. Such changes are regarded seriously by response groups such as Emergency Managers, and the elevated risk levels from SPC resulted in a more intense level of civic and government response (Morris et al. 2002) to this potential tornado threat. In fact, NOAA's Service Assessment Report for the 3 May 1999 tornadoes (NWS 1999) noted the critical role that the profiler data had in improving the forecasts (Convective Outlooks and Watches) from the SPC, and recommended that the existing profiler network be supported as a reliable operational data source. (S. Weiss, personal communication)

The National Weather Service Forecast Office in Sioux Falls, South Dakota, described a wintertime application of profiler data: "Tonight the profiler network was useful for determining the end time of snowfall which coincided with the mid-level trough passage. We had a main trough passage produce up to 6 inches [of snow] and a secondary trough produce areas of IFR [Instrument Flight Rules] conditions but no accumulating snow. The profilers are used almost daily by the forecasters in this office." (P. Browning, personal communication)

The two previous paragraphs described examples of wind profiler data use by operational forecasters. In this article, we discuss the use of profiler data in both numerical weather prediction (NWP) and subjective weather forecasting in three aspects. First, a series of experiments was performed using the Rapid Update Cycle (RUC) model and hourly assimilation system (Benjamin et al. 2004a,b) for a 13-day period in February 2001 comprised of a control experiment with all data and a series of denial experiments in

which different sets of observations were withheld. Data denial experiments were conducted denying profiler and aircraft data. For the control and denial experiments withholding profiler, aircraft, and all data, average verification statistics for RUC wind forecasts against radiosonde observations were compiled for the test period. The day-to-day differences in these errors and in profiler impact were also calculated. In addition to the average RMS wind vector errors, statistics were compiled for the 5% largest errors at individual radiosonde locations to focus on the impact of data denial for *peak* error events. Significance tests were performed for the difference between experiments with and without profiler data.

Second, three case studies illustrating the positive impact of profiler data on RUC forecasts are discussed briefly in section 3 and in more detail in an online supplement. For each case study, reruns of the RUC with and without profiler data are contrasted. The first case is derived from RUC forecasts of the 3 May 1999 Oklahoma tornado outbreak. The second case study is taken from the 13-day test period for a significant snow and ice storm that affected parts of Oklahoma, Kansas, Nebraska, and Missouri on 9 February 2001. The third case is for a tornadic event in central Oklahoma on 8 May 2003 that closely followed the track of the most destructive tornado on 3 May 1999.

2. Data Denial Experiments using the RUC Model

Observation system experiments (OSEs) have been found very useful to determine the impact of particular observation types on operational NWP systems (e.g., Graham et al.

2000, Bouttier 2001, Zapotocny et al. 2002). Four multiday RUC experiments (or OSEs) with assimilation of different observational mixes were performed for the 4–17 February 2001 period. This 13-day period was characterized by strong weather changes across the U.S. and has been used for retrospective testing at the National Centers for Environmental Prediction (NCEP) for modifications to the Eta and RUC model systems. During this period, at least three active weather disturbances traversed the profiler network, including the severe ice and snow that affected parts of the U.S. central plains on 8-9 February 2001. This case is discussed in more detail in section 3.

a. Experimental design

The version of the RUC used in these experiments is the 20-km version run operationally at NCEP as of June 2003, including 50 hybrid isentropic-sigma vertical levels and advanced versions of model physical parameterizations. An hourly intermittent assimilation cycle allows full use of hourly profiler (and other high-frequency) observational data sets. The analysis method is the three-dimensional variational (3DVAR) technique (Devenyi and Benjamin 2003, Benjamin et al. 2003) implemented in the operational RUC in May 2003. Additional information about the 20-km RUC is provided by Benjamin et al. (2002, 2004a,b). The experiment period began at 0000 UTC 4 February 2001 with the background provided from a 1-h RUC forecast initialized at 2300 UTC 3 February. Lateral boundary conditions were specified from the NCEP Eta model initialized every 6 h and available with 3-h output frequency. The high-frequency observations used include those from wind profilers, commercial aircraft, Doppler radar

velocity azimuth display (VAD) wind profiles, and surface stations. No RASS (Radio Acoustic Sounding System, e.g., Martner et al. 1993) temperature profiles, also available at many NPN sites (Fig. 1), were used in any of these experiments since they are not yet available in the operational data stream at NCEP.

Verification was performed using conventional 12-hourly radiosonde data over the three domains depicted in Fig. 2. The entire RUC domain contains ~90 radiosonde sites. The solid box outlining the profiler subdomain includes most of the Midwest profilers depicted in Fig. 1 and contains 22 radiosonde sites. The dashed box area in Fig. 2, referred to as the "downstream" subdomain, contains 26 radiosonde sites. It was chosen to depict an area that might be affected due to downstream propagation of information originating from the profiler data. For each RUC experiment, residuals (forecast minus observed) were computed at all radiosonde locations located within each respective verification domain. Next, the rms (root mean square) vector difference between forecasts and observations was computed for each 12-h verification time. This difference is sometimes referred to below as 'forecast error', but in fact also contains a contribution from observation error (including representativeness "error" from the inability of a grid to resolve sub-grid variations sometimes evident in observations). These scores were then averaged linearly over the 13-day test period. In many of the figures that follow, the statistic displayed is a *difference* between these average scores: the control (RUC run with all data, henceforth referred to as CNTL) minus the experiment (no profiler, no aircraft, or no observations at all; henceforth referred to as EXP). In addition, the student *t* test was performed on the differences between the CNTL and EXP standard deviations

of the residuals to determine statistical significance of the results. Finally, the mean differences were normalized by three different methods to clarify their contribution to forecast error, as described in section 2f. Quality control flags from RUC analyses in the CNTL cycle were applied to verifying radiosonde data.

b. Control experiment

We first consider rms wind differences from radiosonde observations for RUC forecasts from the control experiment with all observational data included. Figure 3 shows the rms wind vector difference between 3-h and 6-h RUC forecasts and radiosonde observations by mandatory level averaged over the 13-day period. Results for both the CNTL (all data) and EXP (no profiler, discussed in next section) experiments are shown. These statistics are only for the 22 radiosondes within the profiler subdomain (Fig. 2). Three-hour forecasts show an improvement of about 0.2-0.7 m s^{-1} over 6-h forecasts valid at the same time, corresponding to the benefit of assimilating more recent observations (Benjamin et al. 2004a). The typical peak of rms wind vector error is evident at near-tropopause jet levels, where wind speeds are highest. The fit of the RUC analysis to rawinsondes is also shown in Fig. 3, corresponding approximately to expected observation error and, therefore, equivalent to a 'perfect' forecast. This statistic will be used in one of the score normalizations described in section 2.f.

c. Profiler data denial results

In this section, we discuss results from the difference between the control experiment and an experiment in which all wind profiler data were withheld. Figure 4 shows the average 3-h, 6-h, and 12-h wind forecast impact (EXP – CNTL) results for the 4-17 February test period (rms vector score from each radiosonde verification time averaged over period) for the three different verification domains. This score, reflecting impact of wind profiler data, is positive for all levels and all domains. As expected, the greatest impact at 3 h is evident over the profiler subdomain (Fig. 4b), from 0.3 – 0.6 m s^{-1} at all mandatory levels (850-150 hPa), with an average value of 0.46 m s^{-1} (Table 1). By contrast, the 3-h vertically averaged impact is 0.28 m s^{-1} over the downstream domain and 0.21 m s^{-1} over the full RUC domain. In general, the impact decreases with increased forecast projection. The 12-h forecast impact is quite small over the three verification domains (<0.1 m s^{-1}). (Plots of wind forecast error from different RUC forecasts for a particular case are shown in Benjamin et al. (2004b, Fig. 11), illustrating that differences in rms vector error of ~0.5 m s^{-1} are easily apparent in visual inspection.)

A stratification of profiler impact results by time of day over the profiler subdomain (Fig. 5) revealed that the profiler impact is stronger at 1200 UTC than at 0000 UTC at most vertical levels . This is likely a result of a lower volume of aircraft data in the 0600-0900 UTC nighttime period than the 1800-2100 UTC daytime period (3-h periods preceding the initial time for 3-h forecasts valid at 1200 or 0000 UTC). It also shows that the profiler data can contribute strongly to improving wind forecast at near-tropopause jet levels and that the accuracy of 3-h jet-level wind forecasts valid at 1200 UTC over the United States is strengthened by wind profiler data.

The statistical significance of mean absolute (not rms) CNTL-EXP differences for 3-12-h forecasts by mandatory levels is examined with student-t tests in Table 2. The difference between 3-h forecasts with and without profiler data is statistically significant at the 99% confidence level for the 700-400 hPa levels. The difference for 6-h forecasts was significant at the 80% level or higher at three levels in the profiler and downstream domains and at 5 of 8 mandatory levels over the full RUC domain.

In considering multi-day experiments to test forecast impact from some change, a problem with any long-period average statistic is that it may mask the potentially more significant impact associated with larger errors in active weather events. In Fig. 6, a time series is shown of the 3-h RUC and persistence forecast 500-hPa wind vector errors from the control experiment at each 12-h verification time. The 3-h persistence forecast is determined simply as the RUC CNTL analysis from 3 h before the verification time. There are three higher error events (over the profiler subdomain) evident in this figure for 5 February, 10 February, and 16 February (Julian dates 36, 41, and 47, respectively), all associated with the passage of strong upper-level waves. The 3-h persistence errors peak much more sharply than the 3-h forecast error, indicating that the rapid changes in the 500-hPa wind field are largely but not completely captured by the model forecasts.

A time series of profiler impact at each 12-h verification time (0000, 1200 UTC) at selected mandatory pressure surfaces (Fig. 7) reveals significant day-to-day variations in the profiler impact. Comparing time series of 500-hPa persistence error (Fig. 6) and

profiler impact (Fig. 7) shows some correlation between larger profiler impact (at 850 hPa on 5 and 10 Feb and at 500 hPa on 16 Feb) and more changeable weather situations. Figure 7 also shows that the time-by-time impact from profiler data is usually positive. Intermittent negative impacts evident in Fig. 7 are attributed to aliasing, which can occur from any in situ observing system.

The impact from denying data on active weather days shown in Fig. 7 underscores the importance of performing case studies. However, it is also possible to stratify statistics to isolate impact for peak error events. The values of the top 5% of the largest CNTL and EXP observation-forecast differences (residuals) were also computed. Residuals at each radiosonde location for every 12-h verification time (0000 and 1200 UTC) were combined for each mandatory level and then ranked from largest to smallest. The effective sample size of this combination of residuals for the entire RUC domain is ~2000 (number of radiosondes per 12 h × 2 launch times per day × 12 days), and ~528 for the profiler verification domain.

The top 5% of the CNTL and EXP residual values for 3- and 6-h forecasts over the profiler domain are shown in Fig. 8. The errors at the top 5% level are about twice as large as the errors shown in Fig. 3. The top 5% level differences between CNTL and no-profiler (EXP) forecasts are also considerably larger (generally 0.5-1.0 m s^{-1}) than the overall average values (only up to 0.3-0.6 m s^{-1}, see Fig 4 and Table 1). This indicates that profiler data have a larger impact for large error cases generally associated with active, more difficult forecast situations. We suggest that this approach is appropriate

for other observation NWP impact studies, since significant reduction of error in difficult situations may justify new observations even if the effect on overall statistics may not appear impressive.

d. Aircraft data denial results

Automated observations from commercial aircraft (mostly reported over the U.S. through ACARS – Aircraft Communication Addressing and Reporting System) are another important source of asynoptic wind observations. There are contrasts and complementarity between aircraft data and profiler data coverage in the central U.S. Aircraft data provide high resolution data at enroute flight levels, generally between 300-200 hPa, and a lesser but still significant amount of ascent/descent profiles (Moninger et al. 2003). Profilers provide hourly (and even 6-min) wind profiles, and, of course, are not dependent on flight schedules and route structures.

In this experiment, all aircraft data at all levels were withheld over the entire RUC domain. The aircraft data denial impact results for wind forecasts over the profiler subdomain (Fig. 9) indicate that these data impact the forecasts most strongly in the upper troposphere (jet levels). The impact is considerably less in the lower troposphere, both because there are fewer ascent and descent reports and because of the influence of the profiler data. The broader coverage of aircraft data than the current profiler network leads to a longer-lasting forecast impact for 6-h and 12-h forecasts. A more complete description of aircraft versus profiler impact is presented in section 2f.

e. All observational data denial results

In order to calibrate the impact of the profiler data on the accuracy of RUC forecasts, a "no data" experiment was performed. In this no-data experiment, the same initial conditions were used as in CNTL and EXP, but no observations were made available after that point to correct model grids over the 13-day period. This experiment was able to more freely drift away from observed conditions and was constrained only by the updated lateral boundary conditions, the same as those used in all other experiments. Since no observations are assimilated in this experiment, it is essentially equal to a 13-day forecast with updated boundary conditions. For this no-data experiment, the rms vector differences (forecast-observed) for 3-h, 6-h, and 12-h forecasts and even analyses (Fig. 10) are essentially equal, which is expected since no observations are available to allow shorter-range forecasts to provide improvement over longer-range forecasts. Also, the scores are much higher (peaking at ~ 12 m s^{-1} at near-tropopause jet levels) than those for the CNTL experiment (Fig. 3, peaking at ~ 7 m s^{-1}).

The difference between the errors from the no-data experiment (Fig. 10) versus the CNTL run (Fig. 3) corresponds to the combined effect of all observational data toward reduction of the overall forecast error with a given set of lateral boundary conditions. In other words, this difference is that between the "worst case" experiment when all data are denied from the RUC and the best-case experiment when all data are available to the RUC. It is notable that results from the no-data experiment are no worse than shown, an

indication of the strong constraint (and damping of observation impact) from given lateral boundary conditions. This difference will be used in the next section (2f) as one way to calibrate the contribution that denying each individual data source has on the total forecast error in the next section. Graham et al. (2000) performed a similar no-data experiment with the same purpose in their global NWP impact experiments.

f. Normalized results for profiler and aircraft data denial experiments

The impact of data denial can be expressed in terms of percentage of forecast error. In this section, we present results for impact of both profiler and aircraft data within the profiler domain, normalized with two different methods. We first calculate percentage impact as:

$$x_1 = \frac{(EXP - CNTL)}{CNTL}, \qquad (1)$$

where EXP is the average score for profiler or aircraft data denial experiments, and CNTL is the average forecast error score for the control experiment with all data. Using the x_1 normalization, profiler data are shown to reduce 3-h wind forecast error by 11-20% in the 400-700 hPa layer (Fig. 11a). The inclusion of aircraft data is shown to be highly complementary in the vertical with the profiler data, accounting for up to 22% of the 3-h forecast improvement at 250 hPa.

A second normalization to determine data impact, the percentage of the total observational data impact provided by a single observation type in the presence of all other observation types, can be computed as

$$x_2 = \frac{(EXP - CNTL)}{(NODATA - CNTL)}, \qquad (2)$$

as discussed in section 2e. This normalization was also used by Graham et al. (2000) for their global OSEs. Normalizing with the no-data vs. control difference (x_2) profiler data accounts for up to 30% (at 700 hPa) of the total reduction of wind forecast error from assimilating all observations (Fig. 11b). Regardless of the normalization, these results show that a significant proportion of the short-range wind forecast skill over the central U.S. is due to profiler data. The inclusion of aircraft data is shown to be highly complementary in the vertical with the profiler data, accounting for up to 20-25% of the 3-h forecast improvement at 250 hPa but much less than profiler data in the 500-850 hPa layer.

Since the forecast-observation difference consists of both forecast and observation error (discussed in section 2.a), we also present profiler impact results (Fig. 11c) for a third normalization, preferred by us since it best accounts for observation error,

$$x_3 = \frac{(EXP - CNTL)}{(EXP - ANX_E)}, \qquad (3)$$

where EXP and CNTL are as described above and ANX_E is the analysis fit to observations (shown in Fig. 3) for the EXP run. This score may be interpreted as the percentage reduction of forecast error produced by some change, assuming that a forecast that fit observations as well as the analysis would be a perfect forecast. By this normalization, profiler data produce a 13-30% reduction of 3-h wind forecast error at all mandatory levels shown from 150-850 hPa. Even though profiler observations are for wind only, they also benefit short-range forecasts of other variables (Fig. 11c): height (error reduction of up to 30%), relative humidity, and temperature. Averaged over mandatory levels, the mean reduction of 3-h forecast error from assimilation of profiler data is 6% for temperature, 5% for relative humidity, 15% for height, and 21% for wind. If RASS temperatures had also been included in the CNTL run (see section 2a), more impact from the profiler/RASS combined observations would likely have been evident in the lower troposphere. This improvement in forecasts of other variables results from the multivariate effects of the RUC analysis and subsequent interaction in the forecast model.

Profiler data have more impact than aircraft data on 3-h wind forecasts in the lower troposphere over the profiler subdomain because there are fewer, less frequent, and less evenly distributed (in a spatial sense) ascent/descent profiles compared to the ~30 profilers within the profiler domain. Figure 12 shows a distribution of ACARS-relayed aircraft observations below 300 hPa for a representative daytime weekday 12-h period from the experiment period. Most of the ascent/descent profiles are found at major airport hubs located primarily on the edges of the profiler subdomain, especially on its eastern edge. The spatial coverage of profiler lower tropospheric wind observations is more

complete (Fig. 1) than that of the ACARS ascent/descent profiles within the profiler domain. However, at jet levels near 200-300 hPa, aircraft observations from enroute flights give better spatial coverage than profiler data.

3. CASE STUDIES

In this section, we present highlights from results for data assimilation/model forecast experiments run for two specific cases of interest. These cases are treated in greater detail in the accompanying online supplement for this article. A third case study (8 May 2003) is also described in the online supplement.

a. 3 May 1999 Oklahoma tornado outbreak

Numerous papers (including the March 2002 issue of *Weather and Forecasting*) describe the significance of the 3 May 1999 Oklahoma City tornado outbreak. Edwards et al. (2002) and Thompson and Edwards (2000), writing from the standpoint of operational forecasting, specifically mention the profiler data as an important data source that helped in the diagnosis of the pre-storm convective environment, as previously discussed in section 1. The 20-km RUC with a 1-h assimilation cycle was rerun for the 24-h period (0000 UTC 3 May - 0000 UTC 4 May 1999) with (CNTL) and without (EXP) wind profiler data to assess their impact on forecasts of pre-convective environment parameters and precipitation over Oklahoma.

Prompted by the remarks of Thompson and Edwards (2000), we examined the difference between upper-level wind analyses and forecasts in the CNTL and EXP runs beginning at 1500 UTC. SPC forecasters had noted that a jet streak associated with a deepening trough approaching Oklahoma from the west was underforecast by model runs initialized at 0000 UTC 3 May 1999. They based their assessment on the Tucumcari, New Mexico profiler time/height time series (Fig. 13) showing increasing winds in the 4-10-km layer, with 300-hPa winds increasing from 30 m s^{-1} at 1200 UTC to 50 m s^{-1} within 7 h. In the RUC 6-h forecasts initialized at 1800 UTC (Fig. 14), the winds are stronger at 300 hPa in the CNTL experiment compared to the no-profiler run by about ~4-6 m s^{-1} over a broad area including western Oklahoma and north-central Texas (vector difference of up to 10 m s^{-1} – Fig. 14d). According to the verifying CNTL analysis at 0000 UTC (Fig. 14c), the profiler data improve the accuracy of the short-range RUC upper-level wind forecast by better capturing the jet streak noted in the Tucumcari profiler observations and its subsequent effect on the upper-level winds over the area of convective development in Oklahoma.

In addition to wind fields, forecasts of convective available potential energy (CAPE, an important parameter indicating instability available to fuel convective storm development) derived from the RUC were also examined from the control and no-profiler experiments. (CAPE is calculated here with averaging of potential temperature and water vapor mixing ratio in the lowest 40 hPa.) Figure 15a shows the difference between control and no-profiler 6-h forecast CAPE forecasts valid 2100 UTC 3 May 1999. Observed CAPE values (Fig 15b – CNTL analysis) are generally large (>4000 J kg^{-1}) in

the area where the first storms formed (see supercell track summary; Fig. 16, upper left inset) in southwestern Oklahoma. The increase in CAPE values (by ~1000 J kg^{-1}) in this area in the CNTL run is primarily the result of an improved location of the axis of maximum CAPE (i.e., a reduction in the phase error). The CAPE forecast improvement from assimilation of profiler data was largely related to an enhanced southeasterly flow of moisture (see Fig. S3 in online supplement) into the area of convective initiation and a westward shift of dryline position, both changes closer to observations.

b. Severe snow and ice storm of 9 February 2001

The 20-km RUC was also used to examine the impact of profiler data for a winter storm that brought a variety of weather to the U.S. southern plains on 8-9 February 2001, including heavy sleet and freezing rain from south-central into eastern Kansas. Short-range (3-h) forecasts s from RUC experiments with (CNTL) and without (EXP) profiler data extracted for a 3-h period of intensifying precipitation (0300-0600 UTC 9 Feb 2001) from the 13-day experiment described in section 3 were examined to determine how the profiler data affected the precipitation forecasts. For comparison with 3-h precipitation forecasts, 3-h METAR precipitation observations and radar reflectivity were examined. Several profiler stations in Oklahoma and southern Kansas (see Fig. 1) were well located to capture the flow above and below a frontal zone located in this region, with isentropic lift resulting from overrunning of the frontal zone being a key mechanism for precipitation in the cold sector in this case. By 0000 UTC 9 February, a band of heavier snow was located across west-central Kansas, while sleet and freezing rain intensified

over south-central Kansas. This intensification continued over the next six hours. By 0600 UTC (Fig. 17), radar reflectivity indicated a band of heavier precipitation extending from west-central Oklahoma to northeastern Kansas (including widespread reflectivity > 40 dBZ), with many 3-h METAR precipitation reports from 7-14 mm (0.28-0.56 in) in this zone.

The RUC precipitation forecasts (Fig. 18) for this 3-h period show that the CNTL experiment was more intense (7-12 mm) throughout this frontal zone than in the no-profiler experiment (4-9 mm). The CNTL forecast more closely matched observed 3-h precipitation and radar reflectivity, especially from western Oklahoma into south central Kansas. The difference in precipitation between the two experiments was apparently related to the lower-tropospheric frontal position and slope. A three-dimensional analysis of wind flow responsible for these differences in precipitation, including comparisons of vertical cross sections of horizontal and vertical velocity and hydrometeors, is presented in the online supplement.

SIDEBAR in BAMS article: Use of Profilers by Operational Forecasters

Wind profiler data are used regularly by National Weather Service (NWS) forecasters. Forecasters typically use a time series display of hourly profiler winds and also display overlays of profiler winds on satellite and/or radar images to better discern mesoscale detail. In addition, profiler data are often used to help verify analyses and short-range forecasts from the models, enabling forecasters to judge the reliability, in *real time*, of the

model guidance. NOAA Profiler Network (NPN) profilers are located near many WFOs in the Central and Southern Regions of the NWS. (Also, boundary-layer profilers located near each coast, not used in NWP tests described here, are used by Western and Eastern Regions of the NWS.) In 2002, The NWS Southern Region Scientific Services Division conducted a survey for WFOs within the NPN area to inquire how the profiler data are used in operations. Forecasters noted that they use profiler data for synoptic analysis, evaluation of model guidance, mesoscale analysis, discerning short-term changes, checking the prestorm environment, monitoring evolving upper-level jet streaks, and for low-level jet (LLJ) detection and monitoring moisture advection with the LLJ. Forecasters described more specific instances in which profiler data were used, and some of these are given below:

- Topeka and Wichita (Kansas) WFOs - Monitoring a rapidly evolving low-level shear profile that resulted in conditions favoring supercells, which enabled the forecasters to be well-prepared in anticipating the tornado outbreak on 19 April 2000. The Neodesha (KS) profiler showed a vertical speed/directional shear profile developing rapidly over a 3-6 hour time period that was ideal for tornadic storms. Mesoscale data including profilers were used to put out an accurate and specific nowcast about exactly where severe convection would develop in the next 1-hour period.
- Amarillo (Texas) WFO
    - Forecasting high wind events by monitoring strong above-surface winds in the Texas and Oklahoma Panhandles

    - Forecasting cold air fronts through high-frequency monitoring of depth and strength of cold air surge possible only with profiler data
    - Monitoring low-level jets and low-level wind shear profiles important for forecasting thunderstorm outbreaks and possible rotating storms and tornadoes.
- Topeka (Kansas) WFO - Ending a winter weather warning. Profiler data confirmed that placement of an upper-level low in the models was incorrect, and the warning was cancelled much sooner than it otherwise would have been.
- Albuquerque (New Mexico) WFO – Specialized weather forecasting for fires near Albuquerque. Wind observations from the Tucumcari profiler helped forecasters to accurately predict a midnight wind surge that led to a fire blowup. Fire fighters were therefore prepared and able to contain the fire during intensification.

While the 3 May 1999 case was a dramatic example of profiler data use at the NOAA Storm Prediction Center (see beginning of this article), SPC forecasters often use profiler data on an hourly basis. The impacts/uses of profiler data at the SPC are summarized below:

- Needed to reliably diagnose changes in vertical wind shear at lower levels (< 3 km above ground level) as well as through a deep layer (through 6 km AGL), both critical to determining potential tornado severity
- Used to better determine storm motion, critical in distinguishing stationary thunderstorms that produce flooding from fast-moving thunderstorms that produce severe weather.

- Used to better determine storm relative flows, and consequently the character of supercells (HP (heavy precipitation) vs. classic)
- Critical for monitoring the low-level jet life cycle, an important factor in MCS (mesoscale convective system) development and therefore the threat for flooding and/or severe weather.
- Unique in providing high-frequency full-tropospheric winds compared with radiosonde and VAD data. While Doppler radar-derived VAD winds also provide high frequency, they cannot monitor deeper-layer vertical wind shear, critical information for SPC. The SPC has added use of the 6-min profiler data since 2000 to better monitor conditions with rapidly evolving severe weather.

4. Discussion and Conclusions

The importance of data from the wind profiler network for forecasting in the United States has been documented through data denial experiments with the RUC for a 13-day period from February 2001, three severe storm case studies (3 May 1999, 9 February 2001, and 8 May 2003), and through a summary of the use of profiler data within the National Weather Service. Verification statistics from the RUC profiler data denial experiments shown in this paper demonstrate that profiler data contribute significantly to the reduction of the overall error in short-range wind forecasts over the central U.S. for this Feb 2001 test period. Forecast errors for height, relative humidity, and temperature were also reduced by 5-15% averaged over vertical levels. This contribution from profiler

data is above and beyond the contributions to initial conditions provided by complementary observations from ACARS/aircraft, VAD and surface stations. A significant contribution from profiler data to improved short-range (3-h) forecast accuracy of 12-28% at all mandatory levels from 850-150 hPa was shown from the RUC experiments for the 13-day test period. Moreover a substantial reduction of wind forecast error (~25%) was shown to occur even at near-tropopause jet levels for forecasts initiated at night from assimilation of profiler data.

Comparisons were made between experiments in which profiler data were withheld and a second experiment in which all aircraft data were withheld. The complementary nature of the two types of observations contributing to a composite high-frequency observing system over the United States was evident, with profiler observations contributing more to improvement through the middle and lower troposphere, aircraft observations contributing more strongly at near-tropopause jet levels. The picture is actually more complex, with aircraft ascent/descent data adding full-tropospheric profiles of winds and temperature and profilers contributing high-frequency jet-level wind observations at night, both adding further accuracy to short-range forecasts. Benjamin et al. (2004a), in a detailed description of the RUC and the performance of its assimilation/forecast system, show the effectiveness of the RUC in using high-frequency observations over the United States to provide improved skill in short-range wind forecasts down to as near-term as a 1-h forecast. These accurate short-range forecasts are critical for a variety of users, including aviation, severe weather forecasting, the energy industry, spaceflight operations, and homeland security concerns. Without question, it is the combined effect

of the profiler/aircraft composite observing system that is most responsible for this strong performance in RUC short-range wind forecasts over the U.S.

Profiler observations fill gaps in the ACARS/aircraft observing system, with automated, continuous profiles 24 h per day with no variations over time of day or day of week (package air carriers operate on a much reduced schedule over weekends). Profiler data are available (or could be) when aircraft data may be more drastically curtailed, owing to national security (e.g., 11-13 September 2001) or severe weather events such as the East Coast snowstorm of 15-17 February 2003. Profiler observations also allow improved quality control of other observations from aircraft, radiosonde, radar, or satellite.

Although the average statistical NWP impact results are compelling evidence that the profiler data add value to short range (0-6 h) NWP forecasts, the value ranges from negligible, often on days with benign weather, to much higher, usually on days with more difficult forecasts and active weather. This day-to-day difference was evident in breakdowns of profiler impact statistics to individual days and to peak error events. These breakdowns were made to accompany the cumulative statistics that generally mask the stronger impact that occurs when there is active weather and a more accurate forecast is most important.

Detailed case studies were carried out using the RUC assimilation cycle and forecast model with and without profiler data for three severe weather cases. A fairly significant positive impact was demonstrated for the Oklahoma tornado outbreak cases of 3 May

1999 and 8 May 2003. Wind data from the profilers resulted in an improvement in the forecast CAPE, shear, and precipitation forecasts valid at or near the time of storm development. In the 1999 case, the CAPE forecast improvement from assimilation of profiler data was largely related to an enhanced southeasterly flow of moisture into the area of convective initiation and a westward shift of dryline position. Assimilation of profiler data for the 8-9 February 2001 snow and ice storm case study resulted in a better forecast of the ascent of the lower level southerly flow overrunning a strong cold front, resulting in stronger and broader upward motion. The outcome of assimilating profiler data in this case was a more accurate RUC precipitation forecast in an area of significant sleet and snow in Oklahoma and Kansas north of the surface front.

As summarized in this paper, profiler data are widely used and have become an important part of the forecast preparation process in the National Weather Service. Clearly, the utility of NPN data to local forecast offices is greatest for short-term forecasts and warnings, reflecting the unique high time resolution from profilers. The NPN is capable of providing data with time resolution as high as 6 minutes, and forecasters in the NWS Central Region have only recently begun to access the 6-min data routinely. Early indications are that the utility of profiler data in critical short-fuse warning situations is even further enhanced by the 6-min data.

Profiler data are the only full-tropospheric wind data available on a continuous basis over the U.S., and as discussed above, could possibly be the only such data that would be available during extreme weather events or a national security event that would ground commercial aircraft. Profilers also routinely provide full-tropospheric wind observations

in conditions of full cloud cover that cannot be made from any current or planned satellite system.

The critical improvements provided to short-range model forecasts and subjective forecast preparation from wind profiler data, as documented in this paper, have been available only over the central United States and, to a lesser extent, downstream over the eastern U.S. The NWS Service Assessment Report for the 3 May 1999 tornado case (NWS 1999) recommended full operational support for the existing profiler network. These benefits for forecast accuracy and reliability could be extended nationwide by implementation of a national profiler network, although this needs to be the subject of a cost-benefit analysis. As described earlier, the interests that would obtain a national-scale benefit from such a profiler network include not only severe weather forecasting, but also aviation, energy, space flight, and homeland security.

Acknowledgments

We thank Tom Schlatter, Nita Fullerton and Margot Ackley of FSL for their reviews of this manuscript and Randy Collander and Brian Jamison for contributions to graphics. Dan Smith and Pete Browning of the Scientific Services Divisions in the NWS Southern and Central Regions, respectively, and Steve Weiss of the NCEP Storm Prediction Center contributed the material presented in the introduction and the sidebar .

5. References

Benjamin, S.G., J.M. Brown, K.J. Brundage, D. Devenyi, G.A. Grell, D. Kim, B.E. Schwartz, T.G. Smirnova, T.L. Smith, S.S. Weygandt, and G.S. Manikin, 2002: RUC20 - The 20-km version of the Rapid Update Cycle. *NWS Technical Procedures Bulletin No. 490*. [FSL revised version available through RUC web site at http://ruc.fsl.noaa.gov]

Benjamin, S.G., D. Devenyi, S.S. Weygandt, G.S. Manikin, 2003. The RUC 3-d variational analysis (and post-processing modifications). *NWS Technical Procedures Bulletin* (draft). Available at http://ruc.fsl.noaa.gov/ppt_pres/RUC-3dvar-tpb-May03.pdf .

Benjamin, S.G., D. Devenyi, S.S. Weygandt, K.J. Brundage, J.M. Brown, G. Grell, D. Kim, B.E. Schwartz, T.G. Smirnova, T.L. Smith, G.S. Manikin, 2004a: An hourly assimilation/forecast cycle: the RUC. *Mon. Wea. Rev.*, **132**, 495-518 .

Benjamin, S.G., G.A. Grell, J.M. Brown, T.G. Smirnova, and R. Bleck, 2004b: Mesoscale weather prediction with the RUC hybrid isentropic/terrain-following coordinate model. *Mon. Wea. Rev*., **132**, 473-494 .

Bouttier, F., 2001. The use of profiler data at ECMWF. *Meteor. Zeit*., **10**, 497-510.

Devenyi, D., and S.G. Benjamin, 2003: A variational assimilation technique in a hybrid isentropic-sigma coordinate. *Meteor. Atmos. Phys.*, **82,** 245-257.

Edwards, R., Corfidi, S.F., Thompson, R.L., Evans, J.S., Craven, J.P., Racy, J.P., McCarthy, D.W., and M.D. Vescio, 2002: Storm Prediction Center forecasting issues related to the 3 May 1999 tornado outbreak. *Wea. Forecasting*, **17**, 544-558.

Graham, R.J., S.R. Anderson, and M.J. Bader, 2000. The relative utility of current observations systems to global-scale NWP forecasts. *Quart. J. Roy. Meteor. Soc*., **126**, 2435-2460.

Martner, B.E., D.B. Wuertz, B.B. Stankov, R.G. Strauch, E.R. Westwater, K.S. Gage, W.L. Ecklund, C.L. Martin, and W.F. Dabberdt, 1993: An evaluation of wind profiler, RASS, and microwave radiometer performance. *Bull. Amer. Meteor. Soc*., **74**, 599-614.

Moninger, W.R, R.D. Mamrosh, and P.M. Pauley, 2003: Automated meteorological reports from commercial aircraft. *Bull. Amer. Meteor. Soc*., **84**, 203-216.

Morris, D.A., K.C. Crawford, K.A. Kloesel, and G. Kitch, 2002: OK-FIRST: An example of successful collaboration between the meteorological and emergency response communities on 3 May 1999. *Wea. Forecasting*, **17**, 567-576.

National Weather Service, 1999: Service Assessment – Oklahoma/southern Kansas tornado outbreak of May 3, 1999. 51 pp. [Available from National Weather Service, 1325 East-West Highway, W/OS52, Silver Spring, MD 20910 and at ftp://ftp.nws.noaa.gov/om/assessments/ok-ks/report7.pdf].

Thompson, R.L., and R. Edwards, 2000: An overview of environmental conditions and forecast implications of the 3 May 1999 tornado outbreak. *Wea. Forecasting,* **15**, 682-699.

Van de Kamp, D.W., 1993: Current status and recent improvements to the Wind Profiler Demonstration Network. *26th Int. Conf. Radar Meteor*., AMS, Norman, OK, 552-554.

Weber, B.L., D.B. Wuertz, R.G. Strauch, D.A. Merritt, K.P. Moran, D.C. Law, D.W. van de Kamp, R.B. Chadwick, M.H. Ackley, M.F. Barth, N.L. Abshire, P.A. Miller and T.W. Schlatter, 1990: Preliminary evaluation of the first NOAA demonstration network profiler. *J. Atmos. Ocean. Techol*., **7**, 909-918.

Zapotocny, T.H., W.P. Menzel, J.P. Nelson, and J.A. Jung, 2002: An impact study of five remotely sensed and five in situ data types in the Eta Data Assimilation System. *Wea. Forecasting*., **17**, 263-285.

Table captions.

Table 1. Mean reduction in rms wind vector error (m s^{-1}) from EXP (no-profiler) to CNTL experiments over February 2001 test period, averaged over eight mandatory pressure levels.

Table 2. Significance scores for the difference between CNTL and EXP (no-profiler) mean wind vector errors over three domains for February 2001 test period, calculated over all radiosonde observations (averaging different than shown in Fig. 5, leading to slightly different result). *Prs* is pressure level, *diff* is (CNTL –EXP) average difference, *Siglv* is the significance level exceeded by the student-t score (only values of at least 80% are shown), and *num* is sample size.

Domain	----3h---- mean diff	----6h---- mean diff	----12h---- mean diff
Profiler	0.46	0.25	0.07
Downstream	0.28	0.19	0.06
Full RUC	0.21	0.13	0.03

Table 1. Mean reduction in rms wind vector error (m s^{-1}) from EXP (no-profiler) to CNTL experiments over February 2001 test period, averaged over eight mandatory pressure levels.

NATIONAL DOMAIN

	----3h----		----6h----		----12h---		
PRS	DIFF	SIGLV	DIFF	SIGLV	DIFF	SIGLV	NUM
850	0.08	xxxxx	0.06	xxxxx	0.06	xxxxx	2047
700	0.17	95.00	0.11	85.00	0.05	xxxxx	2226
500	0.15	90.00	0.09	80.00	0.04	xxxxx	2226
400	0.20	95.00	0.10	xxxxx	0.06	xxxxx	2192
300	0.14	80.00	0.15	80.00	0.01	xxxxx	2115
250	0.24	90.00	0.18	85.00	0.04	xxxxx	2011
200	0.23	90.00	0.15	80.00	0.02	xxxxx	1927
150	0.21	85.00	0.12	xxxxx	0.01	xxxxx	1862

PROFILER DOMAIN

	----3h----		----6h----		----12h---		
PRS	DIFF	SIGLV	DIFF	SIGLV	DIFF	SIGLV	NUM
850	0.31	95.00	0.18	80.00	0.13	xxxxx	515
700	0.38	99.00	0.23	85.00	0.14	xxxxx	578
500	0.42	99.00	0.16	xxxxx	0.08	xxxxx	580
400	0.49	99.00	0.15	xxxxx	0.05	xxxxx	575
300	0.35	90.00	0.23	xxxxx	-0.05	xxxxx	547
250	0.29	85.00	0.33	80.00	0.03	xxxxx	513
200	0.45	90.00	0.24	xxxxx	0.04	xxxxx	489
150	0.31	80.00	0.09	xxxxx	-0.04	xxxxx	450

DOWNSTREAM DOMAIN

	----3h----		----6h----		----12h---		
PRS	DIFF	SIGLV	DIFF	SIGLV	DIFF	SIGLV	NUM
850	0.09	xxxxx	0.07	xxxxx	0.10	xxxxx	826
700	0.18	90.00	0.12	80.00	0.09	xxxxx	823
500	0.24	90.00	0.15	80.00	0.10	xxxxx	822
400	0.26	90.00	0.12	xxxxx	0.10	xxxxx	809
300	0.13	xxxxx	0.20	80.00	0.08	xxxxx	777
250	0.27	85.00	0.18	xxxxx	0.01	xxxxx	733
200	0.30	85.00	0.19	xxxxx	0.05	xxxxx	677
150	0.39	90.00	0.21	xxxxx	-0.07	xxxxx	639

Table 2. Significance scores for the difference between CNTL and EXP (no-profiler) mean wind vector errors over three domains for February 2001 test period, calculated over all radiosonde observations (averaging different than shown in Fig. 5, leading to slightly different result). *Prs* is pressure level, *diff* is (CNTL –EXP) average difference, *Siglv* is the significance level exceeded by the student-t score (only values of at least 80% are shown), and *num* is sample size.

Figure captions

Fig.1. NOAA Profiler Network (NPN) site locations as of August 2002. The LDBT2 site in southeastern Texas was not operational for the cases in May 1999 and February 2001 discussed in this paper. RASS (radio acoustic sounding system, Martner et al.) observations, including lower-tropospheric profiles of virtual temperature, were not used in this study.

Fig. 2. The full 20-km RUC domain with terrain elevation (m), with outlines of profiler (solid line) and downstream (dotted line) verification subdomains.

Fig. 3. Rms vector difference between RUC 3-h and 6-h wind forecasts and radiosonde observations over profiler subdomain for 4-17 February 2001 period for CNTL (all observations) and EXP (no profiler) experiments. Also shown is rms vector difference between *analysis* from CNTL experiment and radiosonde observations (leftmost solid line).

Fig. 4. Effects of profiler data denial (no profiler – CNTL) on average RMS vector errors for 4-17 February 2001 over (a) the full RUC domain, (b) the profiler subdomain, and (c) the downstream subdomain. Positive difference indicates that CNTL experiment *with* profiler data had lower rms vector error than the no-profiler experiment.

Fig 5. Diurnal variability of profiler impact (no profiler – CNTL) on rms 3-h wind forecast vector error in profiler subdomain. Same as Fig. 4b but with separate results for 0000 UTC and 1200 UTC.

Fig. 6. Time series of 500 hPa wind rms vector differences between forecasts and radiosonde observations over profiler subdomain for 5-17 February (Julian date 36-48) 2001 period. Values are shown for 3-h RUC forecasts from control experiment (*03h*) and 3-h persistence forecasts (*03p*, using RUC analyses valid at 0900 and 2100 UTC) also from control experiment.

Fig. 7. Difference in 3-h wind forecast rms vector error score over profiler domain between EXP (no profiler) and CNTL (all data) from every 12-h verification time during 4-17 February 2001 (Julian date 35-48) test period at indicated mandatory isobaric levels.

Fig. 8. Top 5% value of observation-forecast events (residuals) over all radiosondes within profiler domain and all verification times. For CNTL and EXP (no profiler) for 3-h and 6-h forecast residuals.

Fig. 9. Difference in rms vector error scores between no-ACARS experiment and CNTL (all data) experiment over the profiler subdomain for the 4-17 February 2001 period.

Fig. 10. Rms vector difference between radiosonde observations and RUC analyses (anx) and 3-h, 6-h, and 12-h wind forecasts over RUC domain for 4-17 February 2001 period for the *no-data* experiment.

Fig. 11. Normalized impact from observation data denial experiments for RUC 3-h forecasts averaged for the 4-17 February 2001 test period for profiler domain. Relative impact from profiler and aircraft data normalized at each level by (a) 3-h control forecast error (x_1), and (b) difference between no-data error and CNTL error (x_2) for 3-h forecast. Also, (c) impact of profiler data for wind, height, temperature, and relative humidity, normalized with x_3 as in section 2f.

Fig. 12. ACARS-relayed aircraft observations below 300 hPa for the 12-h period from 1200 UTC 8 February – 0000 UTC 9 February 2001 within the profiler subdomain.

Fig.13. Tucumcari, New Mexico (TCUM5) profiler time series valid for 1300 UTC 3 May – 0000 UTC 4 May 1999. Wind speed in m s^{-1}, coded by color in legend at bottom.

Fig. 14. 6-h forecasts of 300 hPa wind (m s^{-1}) for CNTL (top left) and EXP (no profiler,top right) initialized at 1800 UTC 3 May 1999 and valid at 0000 UTC 4 May 1999. (lower left) - verifying (CNTL) analysis at 0000 UTC 4 May 1999.

Fig. 15. 6-h CAPE forecast error (forecast – analysis) for a) CNTL (top left), b) EXP (no profiler, top right). c) Analysis (CNTL) valid at 2100 UTC (bottom) 3 May 1999.

Fig 16. Tornado and supercell (upper left) track summary for 3 May 1999 storms. Provided by NWS Forecast Office, Norman, Oklahoma.

Figure 17. Radar reflectivity (0.5° elevation scan, dBZ color scale shown at bottom) valid at 0600 UTC 9 February 2001 and METAR precipitation (in) totals for 3-h period ending 0600 UTC. (From AWIPS).

Fig. 18. Forecast 3-h precipitation (mm) for 0300-0600 UTC 9 Feb 2001 from CNTL (left) and no-profiler experiments (right), forecasts initialized at 0300 UTC.

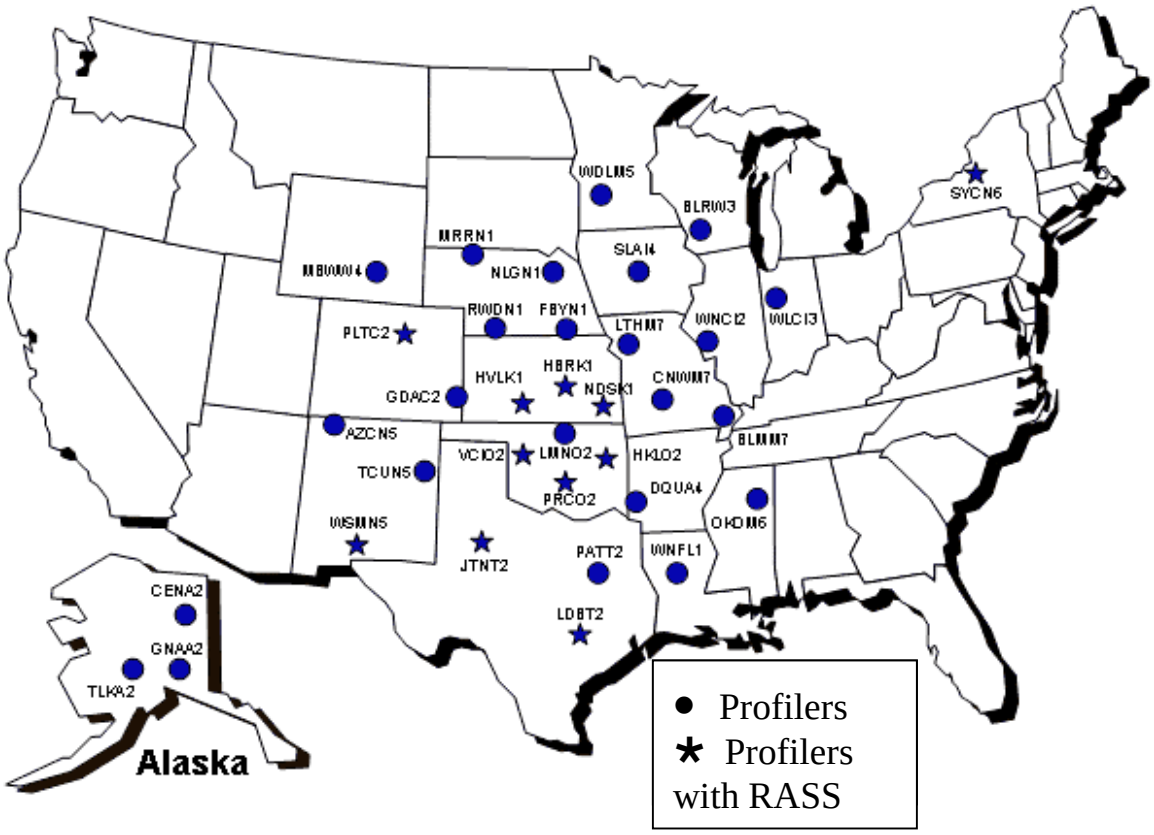

Fig.1. NOAA Profiler Network (NPN) site locations as of August 2002. The LDBT2 site in southeastern Texas was not operational for the cases in May 1999 and February 2001 discussed in this paper. RASS (Radio Acoustic Sounding System, Martner et al.) observations, consisting of lower-tropospheric profiles of virtual temperature, were not used in this study.

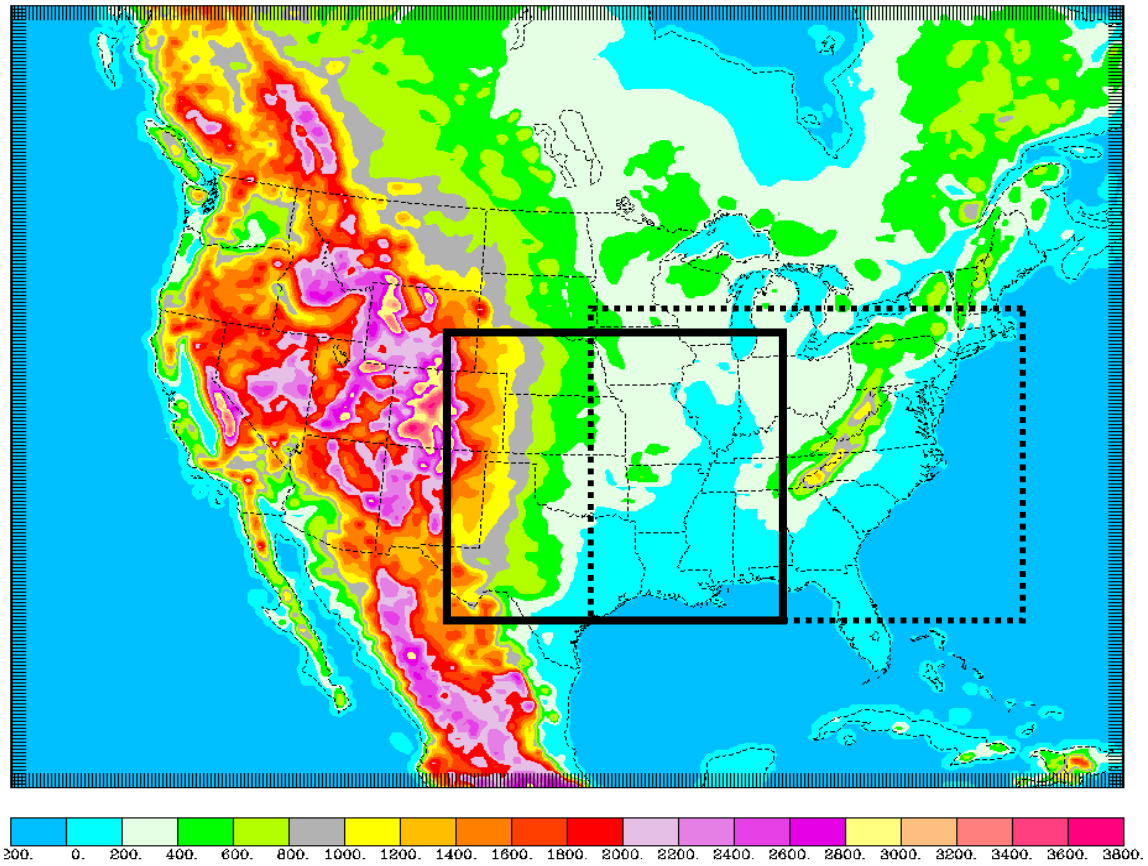

Fig. 2. The full 20-km RUC domain with terrain elevation (m), with outlines of profiler (solid line) and downstream (dotted line) verification subdomains.

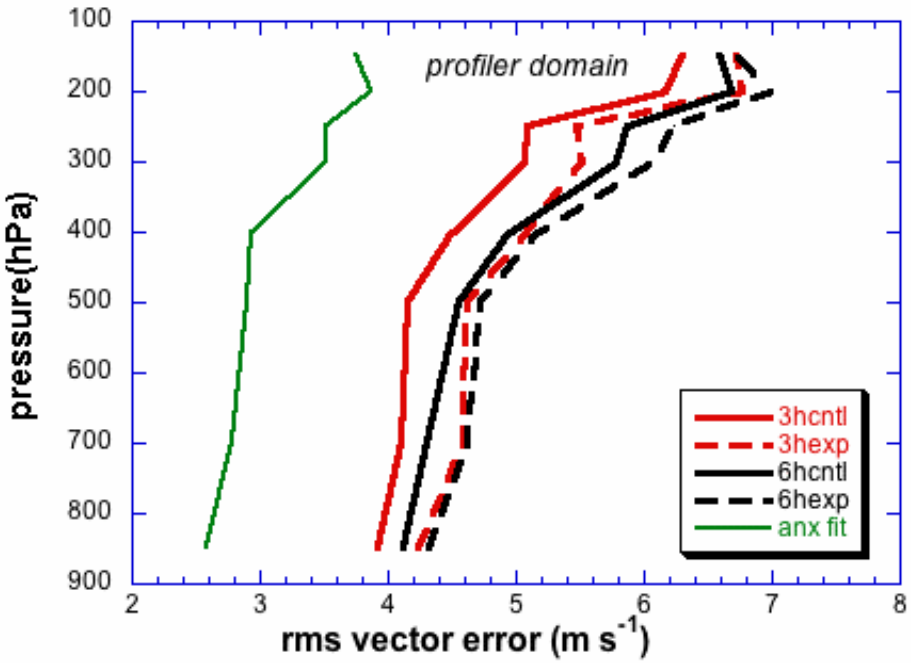

Fig. 3. Rms vector difference between RUC 3-h and 6-h wind forecasts and radiosonde observations over profiler subdomain for 4-17 February 2001 period for CNTL (all observations) and EXP (no profiler) experiments. Also shown is rms vector difference between *analysis* from CNTL experiment and radiosonde observations (leftmost solid line).

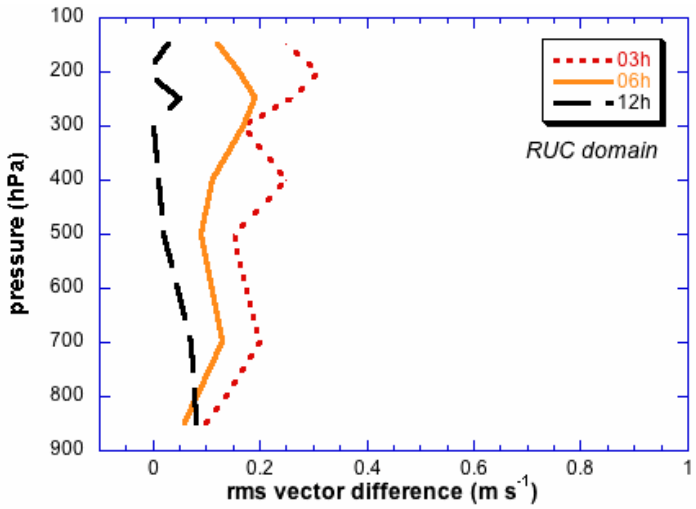
03h
06h
12h
RUC domain
pressure (hPa)
rms vector difference (m s-1)

a)

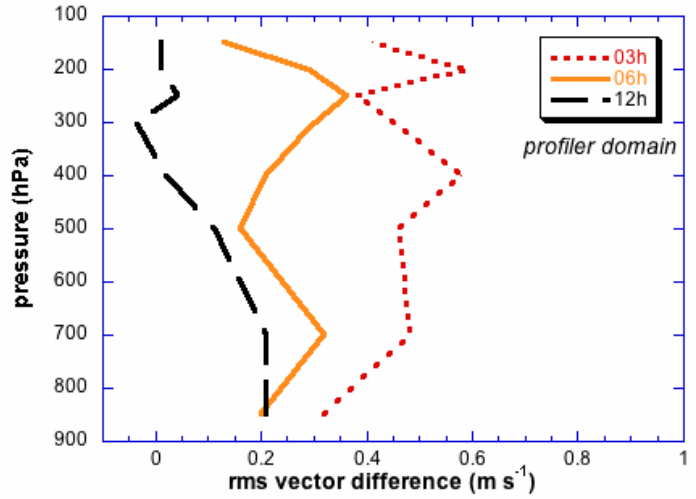
03h
06h
12h
profiler domain
pressure (hPa)
rms vector difference (m s-1)

b)

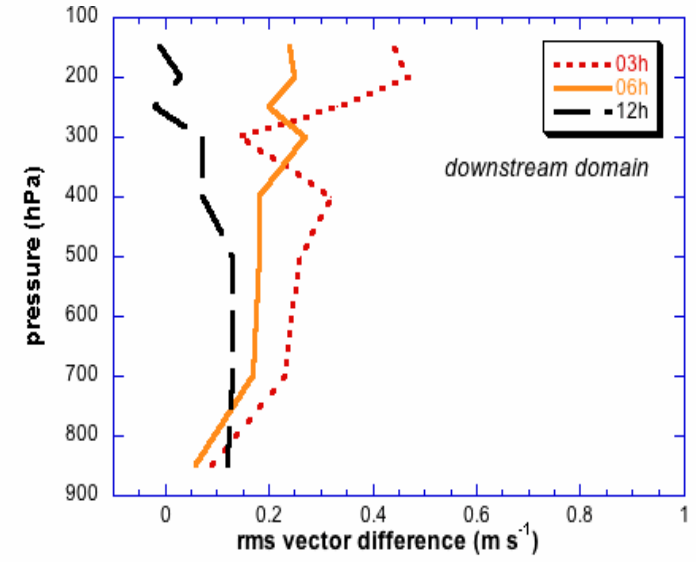
03h
06h
12h
downstream domain
pressure (hPa)
rms vector difference (m s-1)

c)

Fig. 4. Effects of profiler data denial (no profiler – CNTL) on average RMS vector errors for 4-17 February 2001 over (a) the full RUC domain, (b) the profiler subdomain, and (c) the downstream subdomain. Positive difference indicates that CNTL experiment *with* profiler data had lower rms vector error than the no-profiler experiment. Fig. 4b is consistent with the rms vector errors shown in Fig. 3.

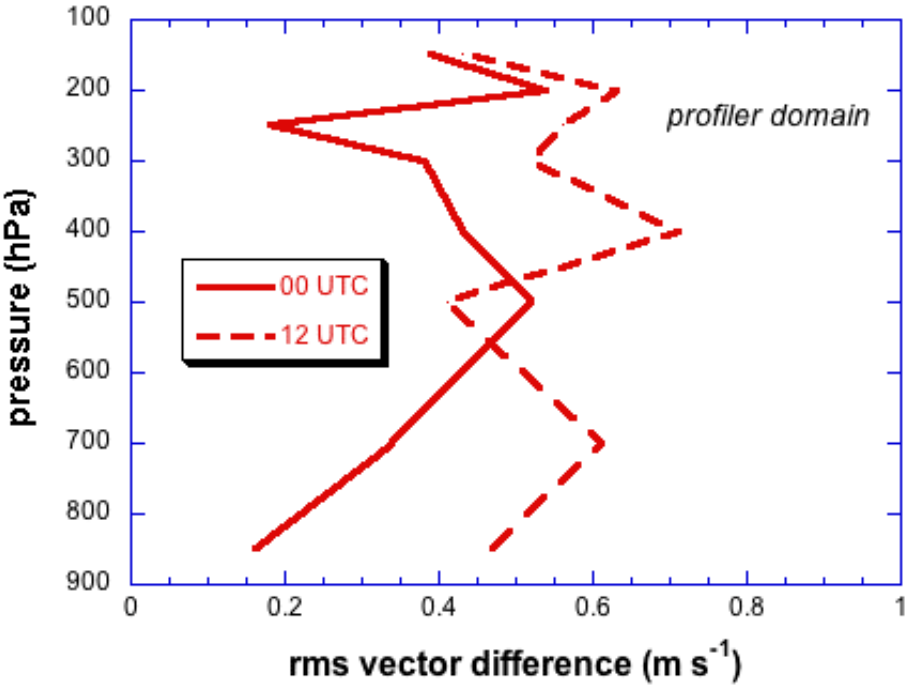

Fig 5. Diurnal variability of profiler impact (no profiler – CNTL) on rms 3-h wind forecast vector error in profiler subdomain. Same as Fig. 4 b but with separate results for 0000 UTC and 1200 UTC.

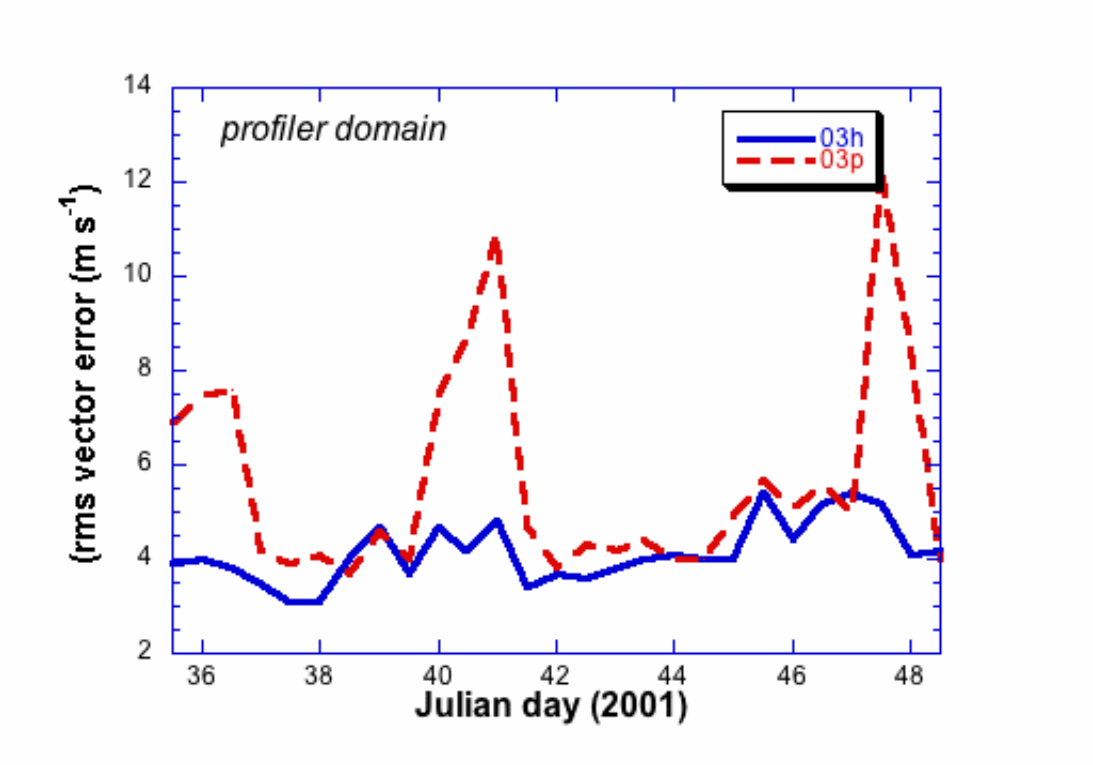

Fig. 6. Time series of 500 hPa wind rms vector differences between forecasts and radiosonde observations over profiler subdomain for 5-17 February (Julian date 36-48) 2001 period. Values are shown for 3-h RUC forecasts from control experiment (*03h*) and 3-h persistence forecasts (*03p*, using RUC analyses valid at 0900 and 2100 UTC) also from control experiment.

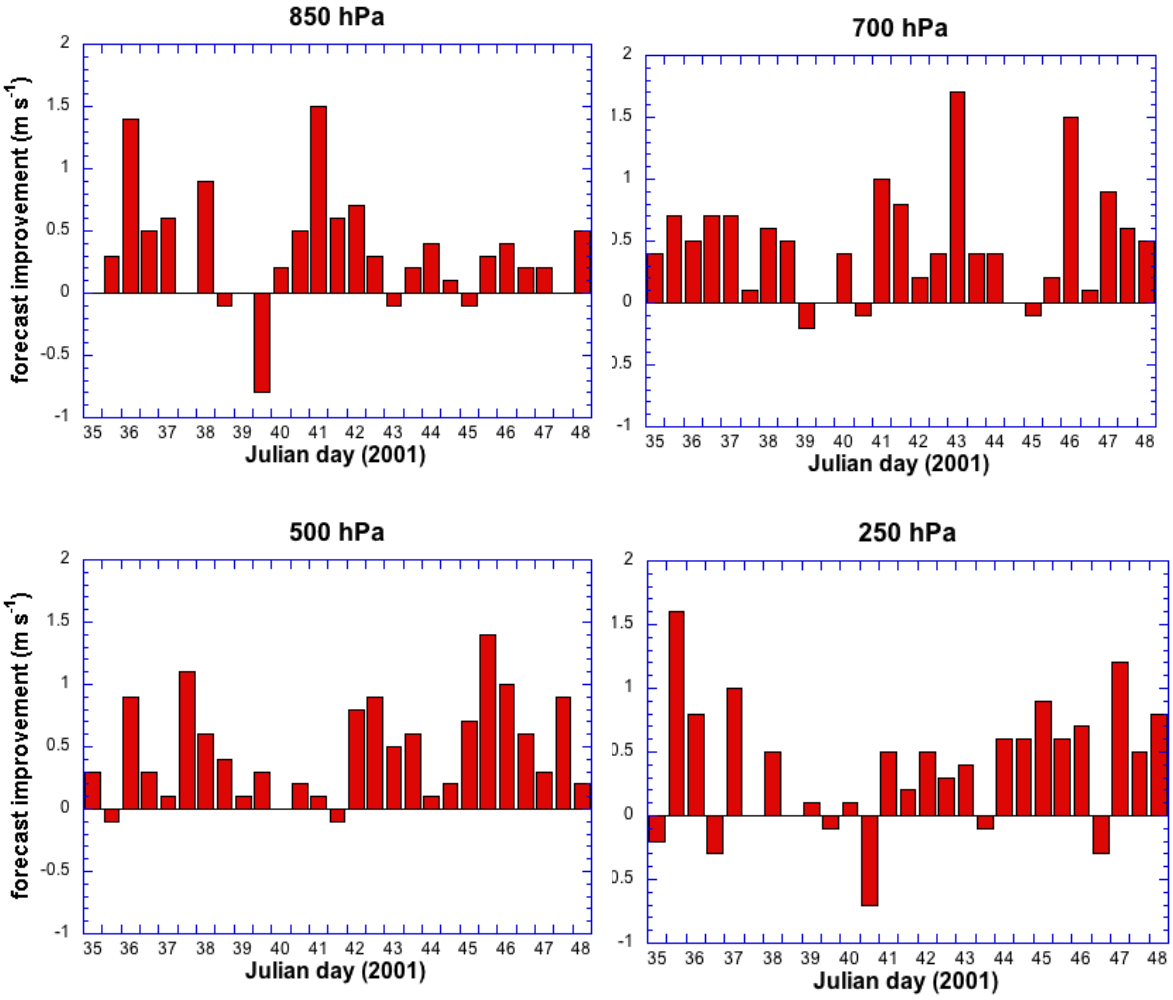

Fig. 7. Difference in 3-h wind forecast rms vector error score over profiler domain between EXP (no profiler) and CNTL (all data) from every 12-h verification time during 4-17 February 2001 (Julian date 35-47) test period at indicated mandatory isobaric levels.

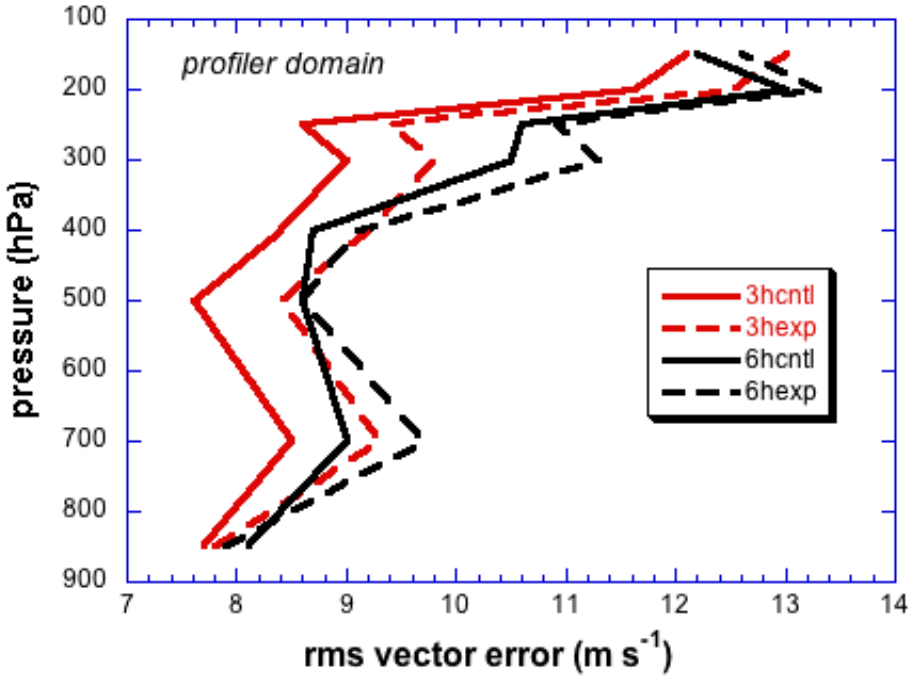

Fig. 8. Top 5% value of observation-forecast events (residuals) over all radiosondes within profiler domain and all verification times. For CNTL and EXP (no profiler) for 3-h and 6-h forecast residuals.

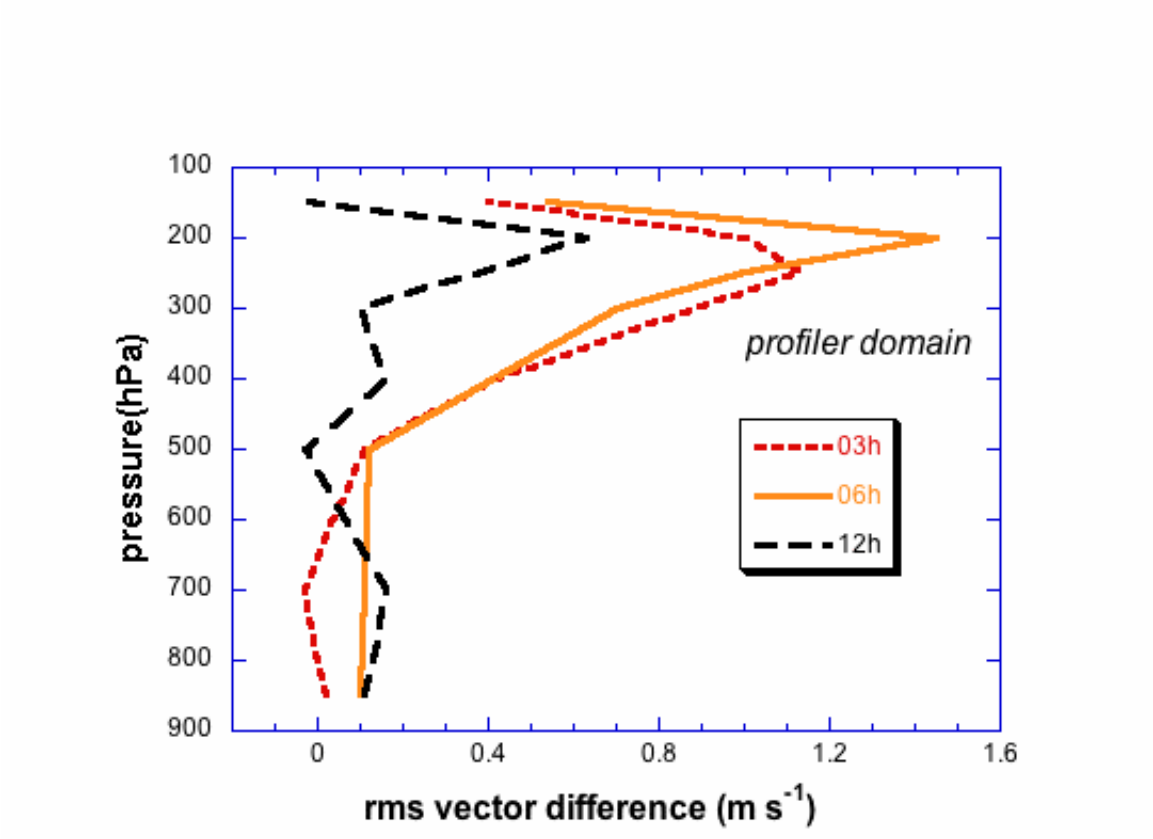

Fig. 9. Difference in rms vector error scores between no-ACARS experiment and CNTL (all data) experiment over the profiler subdomain for the 4-17 February 2001 period.

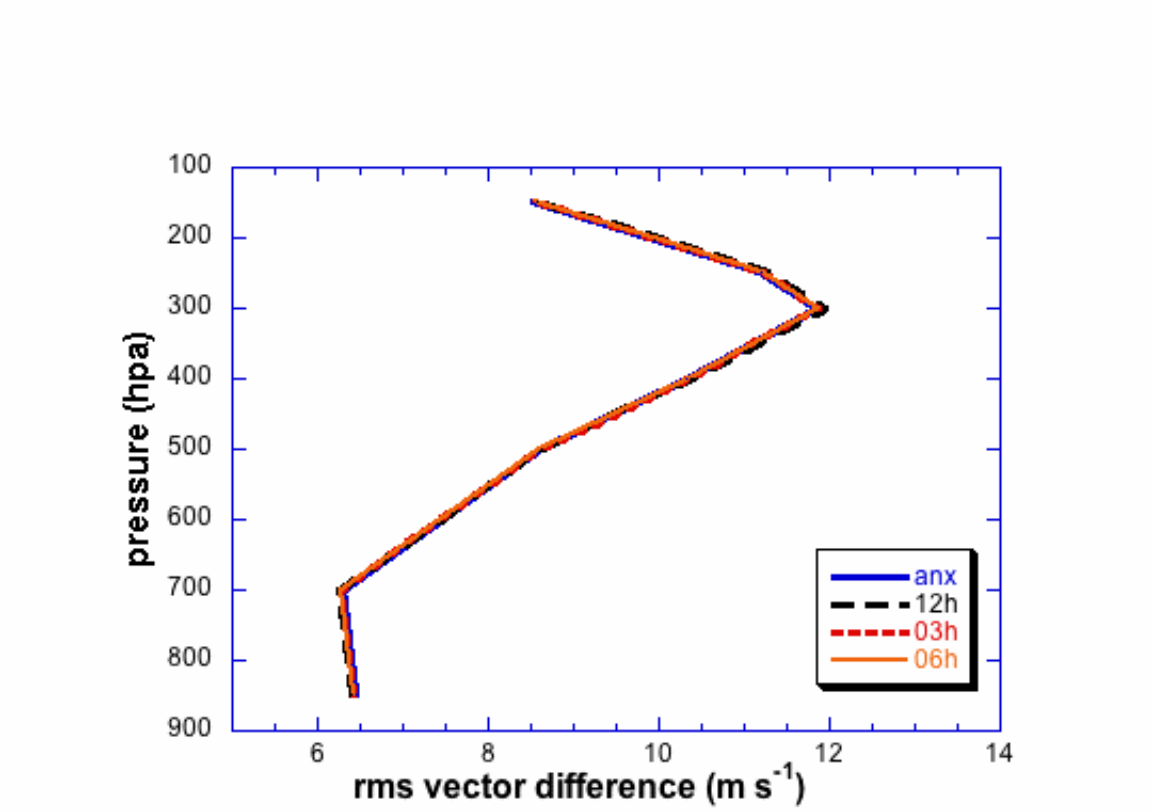

Fig. 10. Rms vector difference between radiosonde observations and RUC analyses (anx) and 3-h, 6-h, and 12-h wind forecasts over RUC domain for 4-17 February 2001 period for the *no-data* experiment.

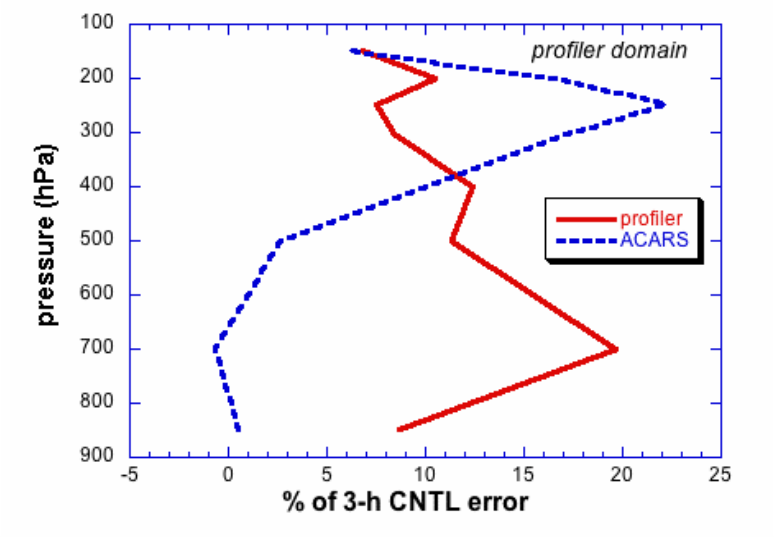
profiler domain
profiler
ACARS
pressure (hPa)
% of 3-h CNTL error

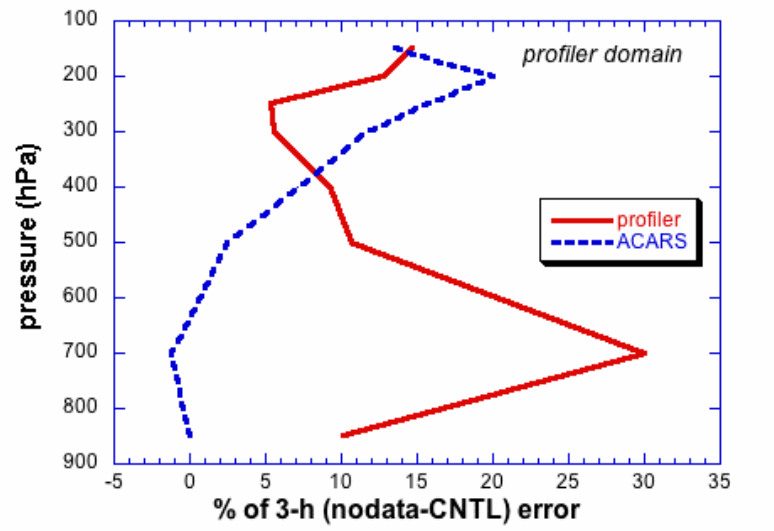
profiler domain
profiler
ACARS
pressure (hPa)
% of 3-h (nodata-CNTL) error

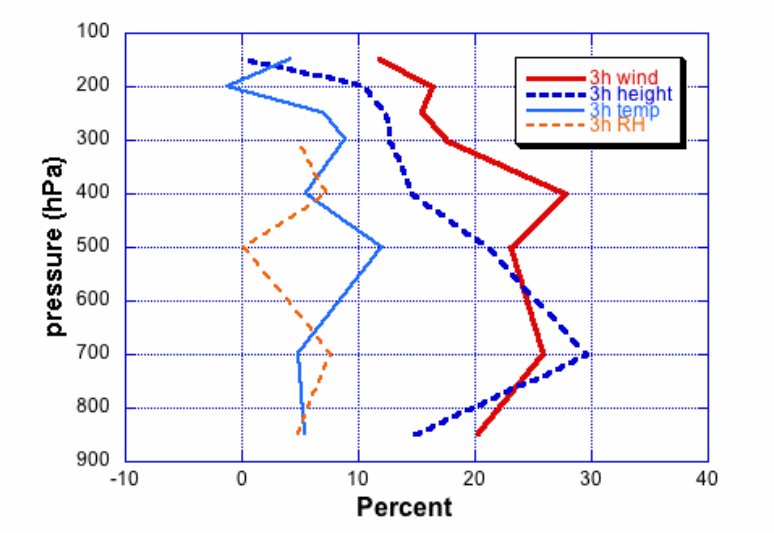
3h wind
3h height
3h temp
3h RH
pressure (hPa)
Percent

Fig. 11. Normalized impact from observation data denial experiments for RUC 3-h forecasts averaged for the 4-17 February 2001 test period for profiler domain. Relative impact from profiler and aircraft data normalized at each level by (a) 3-h control forecast error (x_1), and (b) difference between no-data error and CNTL error (x_2) for 3-h forecast. Also, (c) impact of profiler data for wind, height, temperature, and relative humidity, normalized with x_3 as in section 2f.

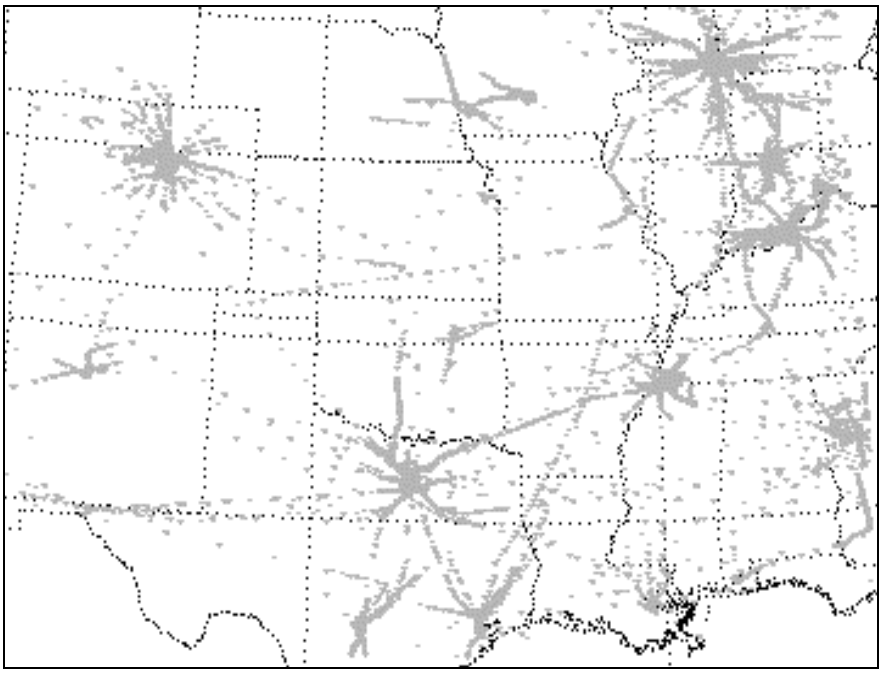

Fig. 12. ACARS-relayed aircraft observations below 300 hPa for the 12-h period from 1200 UTC 8 February – 0000 UTC 9 February 2001 within the profiler subdomain.

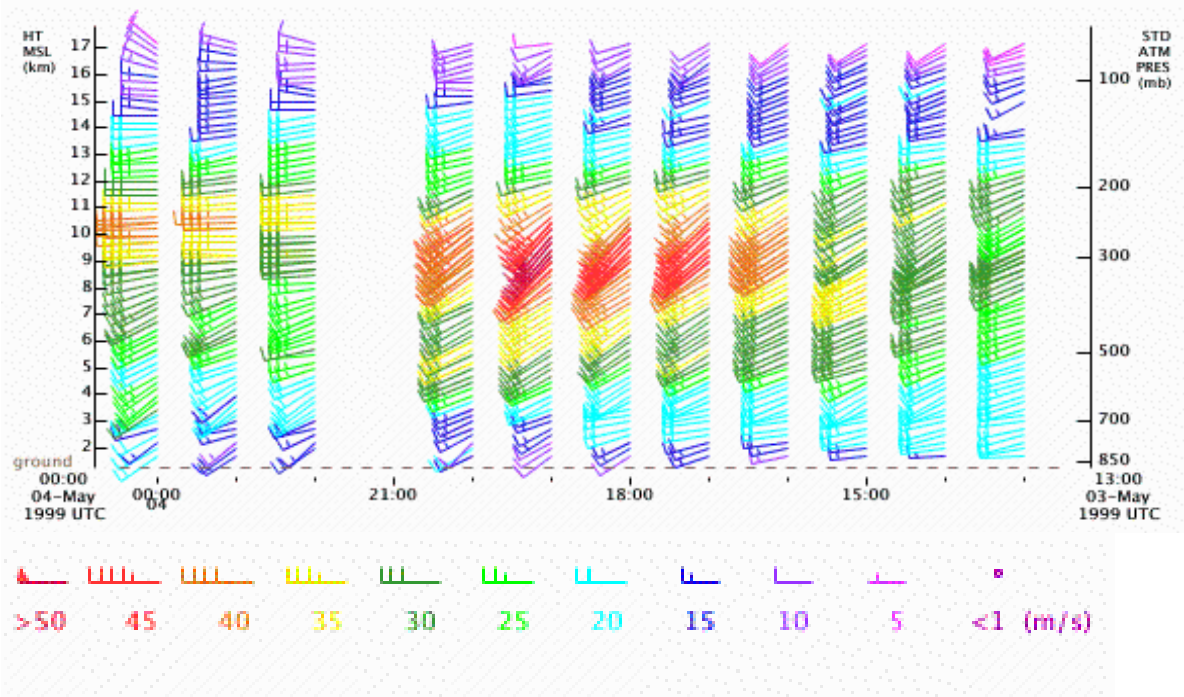

Fig.13. Tucumcari, New Mexico (TCUM5) profiler time series valid for 1300 UTC 3 May – 0000 UTC 4 May 1999. Wind speed in m s^{-1}, coded by color in legend at bottom.

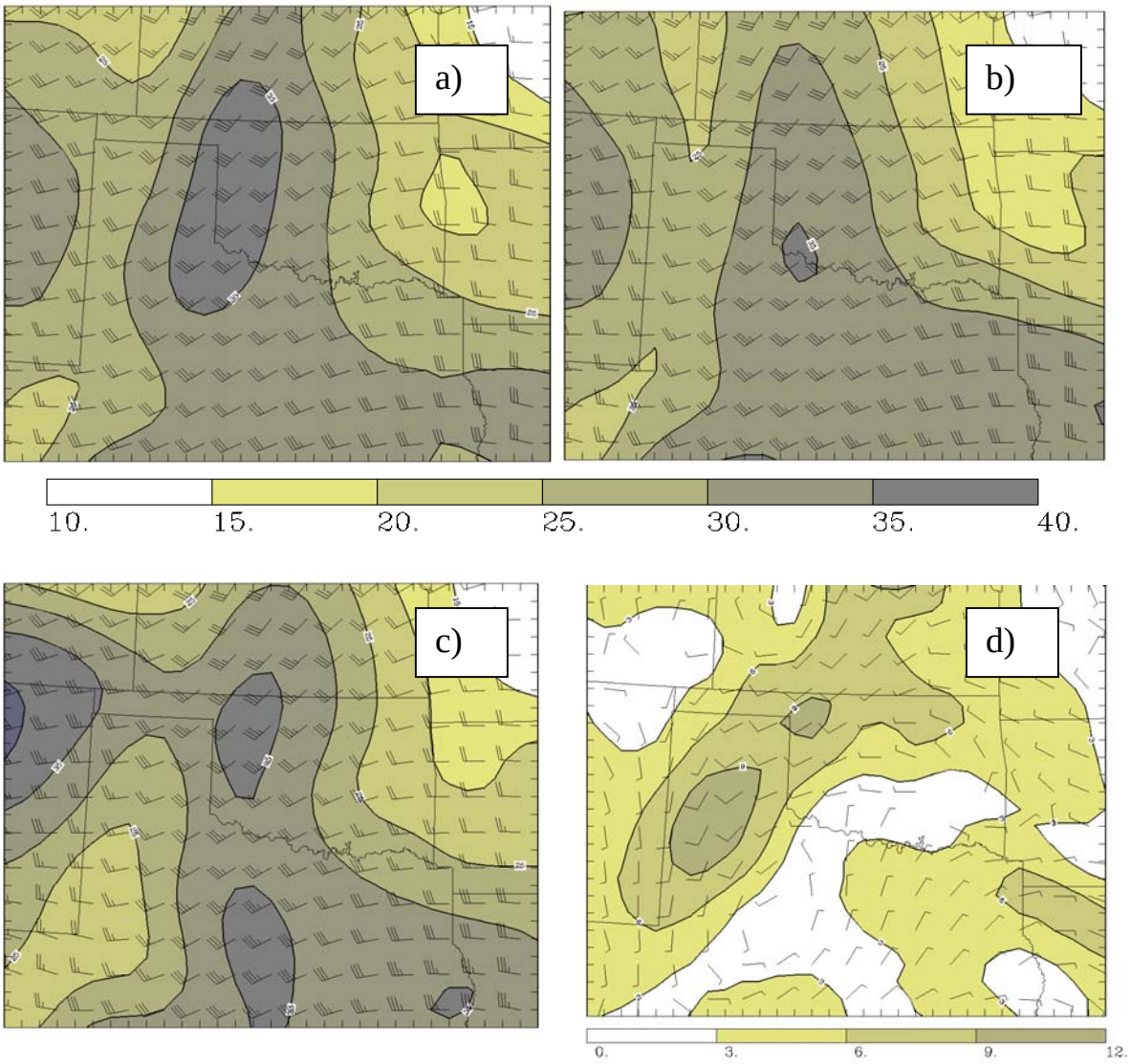

Fig. 14. 6-h forecasts of 300 hPa wind ($m\,s^{-1}$) for a) CNTL (top left) and b) EXP (no profiler,top right) initialized at 1800 UTC 3 May 1999 and valid at 0000 UTC 4 May 1999. c) verifying (CNTL) analysis at 0000 UTC 4 May 1999 (lower left) and d) CNTL-EXP vector difference between 6-h forecasts (a) – b)).

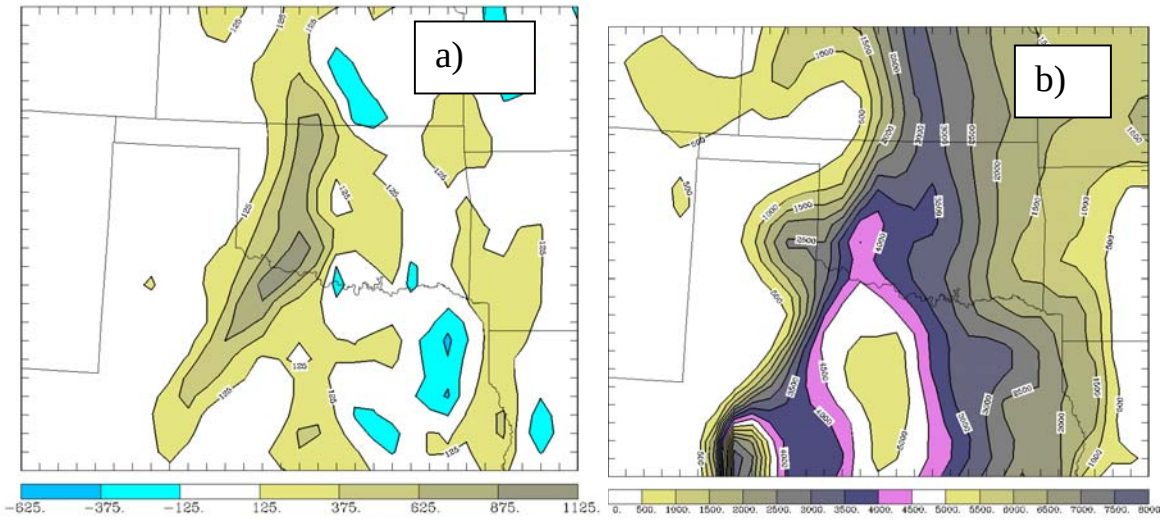

Fig. 15. a) CNTL-EXP difference for 6-h CAPE forecast and b) CAPE values from analysis (CNTL) valid at 2100 UTC 3 May 1999.

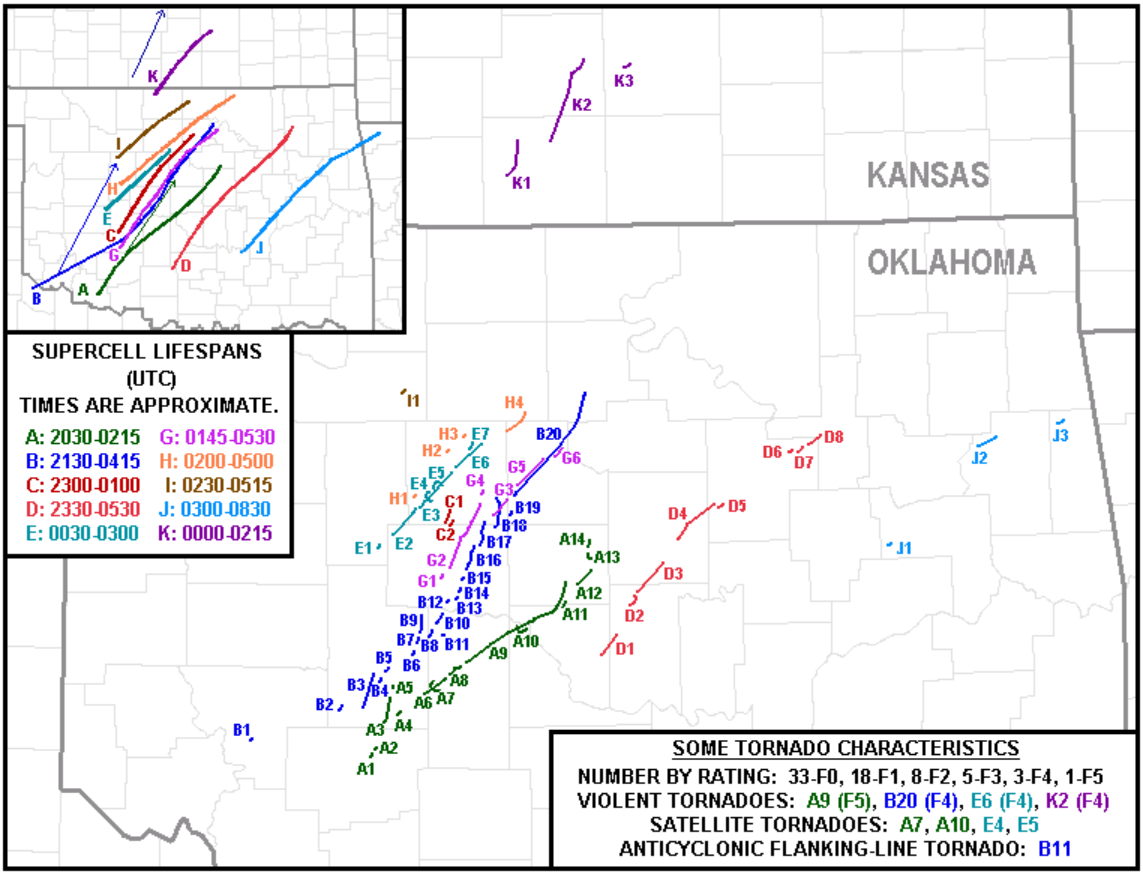

Fig 16. Tornado and supercell (upper left) track summary for 3 May 1999 storms. Provided by NWS Forecast Office, Norman, Oklahoma.

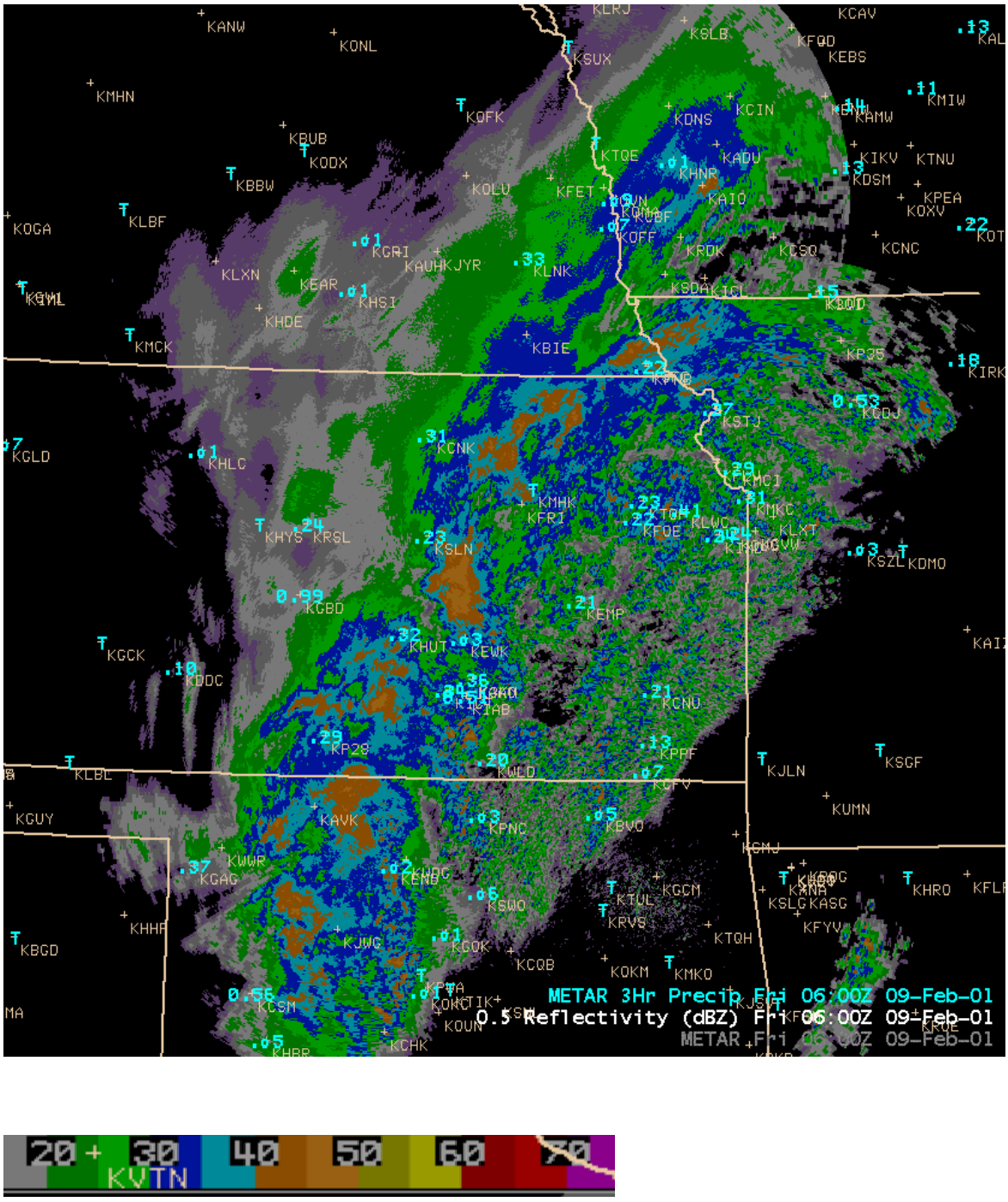

Figure 17. Radar reflectivity (0.5° elevation scan, dBZ color scale shown at bottom) valid at 0600 UTC 9 February 2001 and METAR precipitation (in) totals for 3-h period ending 0600 UTC. (From AWIPS).

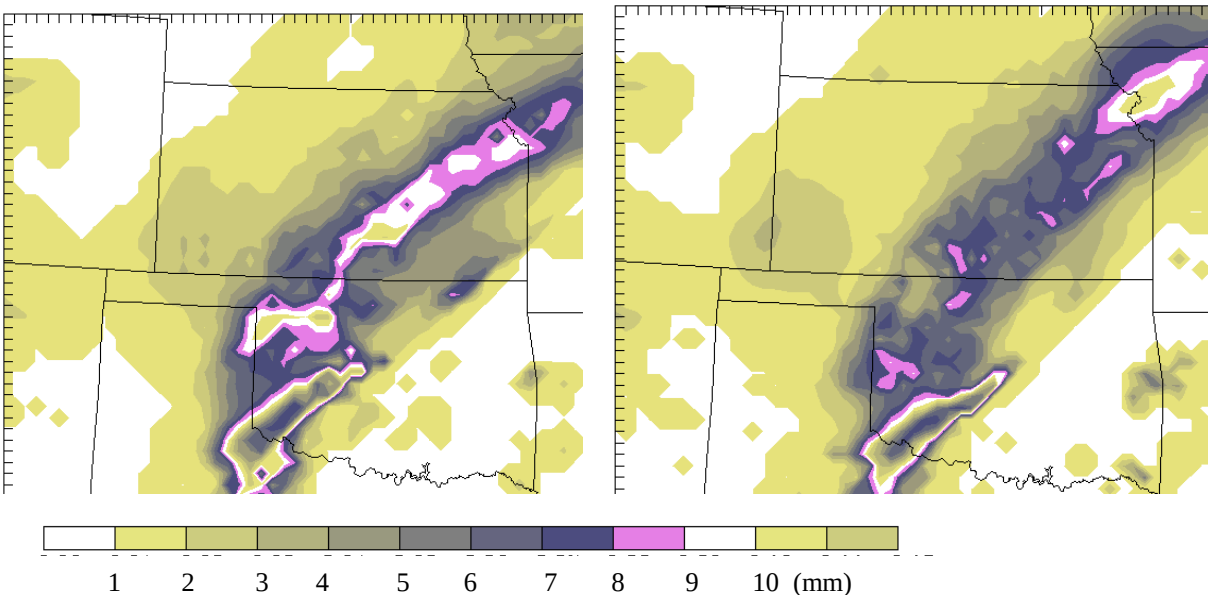

Fig. 18. Forecast 3-h precipitation (mm) for 0300-0600 UTC 9 Feb 2001 from CNTL (left) and no-profiler experiments (right), forecasts initialized at 0300 UTC.

Online Supplement - CASE STUDIES

In this section, we describe in greater detail the two case studies presented briefly in the main paper, plus an additional case study for 8 May 2003.

a. 3 May 1999 Oklahoma tornado outbreak

Numerous papers (including the May 2002 issue of *Weather and Forecasting*) describe the significance of the 3 May 1999 Oklahoma City tornado outbreak. Edwards et al. (2002) and Thompson and Edwards (2000), writing from the standpoint of operational forecasting, specifically mention the profiler data as an important data source that helped in the diagnosis of the pre-storm convective environment. The introduction of the main paper includes remarks of forecasters from NOAA's Storm Prediction Center (SPC) about the importance of profiler data on this day. The 20-km RUC with a 1-h assimilation cycle was rerun for the 24-h period (0000 UTC 3 May - 0000 UTC 4 May 1999) with (CNTL) and without (EXP) the profiler data to assess their impact on forecasts of pre-convective environment parameters and precipitation over Oklahoma. (Profiler observations were not available for operational forecasts from the then-40-km RUC due to computer timing issues for predictions actually run on 3 May 1999. VAD (velocity azimuth display) winds from WSR-88D radars were neither used in the actual RUC predictions for this event nor in this case study due to quality issues identified at NCEP.)

Prompted by the remarks of Thompson and Edwards (2000), we first examined the difference between the wind analyses and forecasts in the CNTL and EXP runs beginning about 1500 UTC. The authors describe an embedded jet streak associated with a deepening trough that was approaching Oklahoma from the west, and how the NCEP Eta model from the 0000 UTC 3 May 1999 run underforecast the intensity of the wind speed maximum aloft (see section 4 of this paper for their complete remarks). They based their assessment on the Tucumcari, New Mexico profiler time/height time series (Fig. S1) showing increasing winds in the 4-10-km layer. The high-frequency profiler data showed 300-hPa winds increasing from 30 m s^{-1} at 1200 UTC to 50 m s^{-1} within 7 h. In the RUC 6-h forecasts initialized at 1800 UTC, the winds are stronger at 300 hPa in the CNTL experiment compared to the no-profiler run by about ~4-6 m s^{-1} over a broad area including western Oklahoma and north-central Texas (Fig. S2). According to the verifying CNTL analysis at 0000 UTC (Fig. S2c), the profiler data improve the accuracy of the short-range RUC upper-level wind forecast by better capturing the jet streak noted in the Tucumcari profiler observations and its subsequent effect on the upper-level winds over the area of convective development in Oklahoma.

The difference between CNTL and EXP 6-h 850-hPa wind forecasts (Fig. S3a) shows an enhancement of the southeasterly flow at low levels related to the CAPE shift evident in Fig. S4a. The general flow at 850 hPa (CNTL analysis at 0000 UTC) is south-southwesterly. The 0-3 km helicity from the CNTL and EXP 3-h forecasts did not show significant difference (not shown). However, the area of maximum helicity (Fig S4c)

from both CNTL and EXP runs was predicted to be centered over the area in southwestern Oklahoma where tornadic storms first formed (Fig. S5).

In addition to wind fields, CAPE forecasts derived from the RUC (with averaging of potential temperature and water vapor mixing ratio in the lowest 40 hPa) were also examined from the control and no-profiler experiments. Figure S4a shows the difference between control and no-profiler 6-h forecast CAPE forecasts valid 2100 UTC 3 May 1999. Observed CAPE values (Fig. S4b) were generally large (>4000 J kg^{-1}) in the area where the first storms formed (see supercell track summary; Fig. S5, upper left inset) in southwestern Oklahoma. The increase in CAPE values (by ~1000 J kg^{-1}) in this area in the CNTL run is primarily the result of an improved location of the axis of maximum CAPE (i.e., a reduction in the phase error). The CAPE forecast improvement from assimilation of profiler data was largely related to an enhanced southeasterly flow of moisture into the area of convective initiation and a westward shift of dryline position, both changes closer to observations. The 3-h CAPE forecast error fields for 2100 UTC (not shown) were similar except that the EXP and CNTL errors were not as large as their 6-h forecast counterparts.

The 3-h and 6-h surface dewpoint forecast error fields (not shown) were consistent with the CAPE error fields, and indicated that dewpoints in the area of the underforecast CAPE in the no-profiler (EXP) were as much as 3ºC lower than in the CNTL run within the area of large EXP CAPE error. A comparison of 850-hPa wind forecasts from the two experiments (Fig. S3) indicated that assimilation of profiler data caused a slight backing

of flow in north and central Texas. The modified 850-hPa flow in the CNTL run with profiler data appeared to cause the extra moisture transport and westward shift in dryline position. The resulting phase shift of the maximum CAPE in the control run with profiler data brought it closer to the region where the storms initiated.

Finally, the supercell track and tornado track summary (Fig. S5) may be compared with the 6-h forecasts of 3-h accumulated precipitation valid at 0000 UTC 4 May from the CNTL and EXP runs (Fig. S6). The initial position of the first supercell (supercell A, see upper left inset in Fig. S5) near the Oklahoma-Texas border is fairly well forecast by both CNTL and EXP experiments. The intensity of the convective precipitation is somewhat more stronger in the CNTL experiment, evidently a result of the higher CAPE associated with the shift in dryline position and backing of low-level flow shown in Figs. S4 and S3.

b. Severe snow and ice storm of 8-9 February 2001

The 20-km RUC was also used to examine the impact of profiler data for a winter storm that brought a variety of weather to the Plains and Midwest on 8-9 February 2001. This event fell within the retrospective test period used for the data denial experiments described in section 2. Although this storm system was fairly typical of winter storms in this area, some locations experienced an impressive storm, with portions of Kansas receiving 25-40 cm (10-16 in) total snowfall (24-h snowfall amounts shown in Fig. S7) and with heavy sleet and freezing rain from south-central into eastern Kansas. Short-range (3-h) forecasts s from RUC experiments with (CNTL) and without (EXP) profiler

data extracted for a 3-h period of intensifying precipitation (0300-0600 9 Feb 2001) from the 13-day experiment described in section 3 (in the main paper) were examined to determine how the profiler data affected the precipitation forecasts. For comparison with 3-h precipitation forecasts, 3-h METAR precipitation observations and radar reflectivity were examined. Several profiler stations in Oklahoma and southern Kansas (see Fig. 1 in main paper) were well located to capture the flow above and below a frontal zone located in this region, with isentropic lift resulting from overrunning of the frontal zone being a key mechanism for precipitation in the cold sector in this case. By 0000 UTC 9 February, a band of heavier snow was located across west-central Kansas, while sleet and freezing rain intensified over south-central Kansas. This intensification continued over the next six hours.

A synoptic overview of the storm is given in Fig. S8. A full-latitude trough moving out of the Rockies placed the Kansas/Oklahoma area in a region of upper-level forcing ahead of the approaching trough. Strong southerly flow was found at the surface south of a sharp, slow-moving cold front located from Kansas City to just west of Oklahoma City at 0000 UTC, stretching back to a surface low in western Texas. Several profiler stations in Oklahoma and southern Kansas (Fig. 1, main article) were located in a good position to capture the southerly flow advecting moisture northward over the front, with overrunning of the frontal zone being a key mechanism for precipitation in the cold sector in this case.

Several waves of precipitation occurred during the daytime hours on 8 Feb, but snowfall was limited to northern and western portions of Kansas (and Iowa and Nebraska), and the

Oklahoma Panhandle. Most of the precipitation over central Kansas fell as freezing rain or sleet before 0000 UTC 9 February, while rain fell over eastern Kansas and southward across most of Oklahoma (except for the Panhandle). By 0000 UTC 9 February, the areas of heavy snow were moving east, with a band of heavier snow across west central Kansas, while sleet and freezing rain intensified over south-central Kansas. Radar reflectivity at 0600 UTC indicated a band of heavier precipitation extending from west-central Oklahoma to northeastern Kansas (including widespread reflectivity > 40 dBZ), with many 3-h METAR precipitation reports from 7-14 mm (0.28-0.56 in) in this zone. (Fig. S9).

The RUC forecasts (Fig. S10) for this 3-h period show that the CNTL precipitation was more intense (7-12 mm) throughout this frontal zone than the no-profiler experiment (4-9 mm). The CNTL forecast more closely matched observed 3-h precipitation and radar reflectivity especially from western Oklahoma into south-central Kansas. The difference in precipitation between the two experiments was apparently related to the lower-tropospheric frontal position, more accurately depicted in the CNTL experiment with profiler data.

A comparison of the analyzed 900-hPa wind fields at 0300 UTC from the CNTL and no-profiler experiments (Fig. S11) helps to explain why the CNTL experiment predicted more precipitation in southern Kansas than the EXP run. The strength of the southerly flow at this level south of the strong cold front, evident as a wind shift, was approximately the same in both experiments. However, the location and curvature of the

front is different. The front in the CNTL experiment is rotated slightly to more of an east-west orientation, giving a sharper ascent to the southerly flow overrunning it. This difference in orientation extends from southwestern Oklahoma into eastern Kansas, including the vertical cross-sections to be shown in Figs. S12-S14. Although these differences are not exceptional, they are important enough to result in heavier forecast precipitation to the north with the CNTL experiment, showing better overall agreement with the observations.

Vertical cross sections from each experiment oriented north-south across the front (Fig. S12), from the 3-h forecast valid at 0600 UTC, show the relationship of the along-flow wind component of 30-35 m s^{-1} south of the front and sloping upward above the front over Kansas. Close inspection reveals the slight shift in frontal position noted in the 900-hPa wind fields in Fig. S12, with a position further north and a sharper ascent of the southerly flow > 30 m s^{-1} north of the surface front in the CNTL experiment. The approproximate position of the axis of heavy precipitation in south-central Kansas north of the surface front is denoted by an arrow in Fig. S12. The flow over the frontal zone ascends more steeply in the CNTL experiment, a consequence of the more east-west orientation of the front noted in Fig. S11. The steeper ascent in the CNTL experiment is evident in a stronger and deeper plume of vertical velocity (Fig. S13) associated with the heavier precipitation over southern Kansas (about 200 km north of the surface front). Upward vertical motion (diagnosed in the RUC model as described by Benjamin et al. 2004b) producing this precipitation is much broader and deeper in the CNTL experiment (note extensive area with greater than 30 μb s^{-1}). Finally, a comparison (Fig. S14)

between CNTL and no-profiler experiments is presented for vertical cross-sections of combined hydrometeor mixing ratio from rain, snow, and graupel, all forecast explicitly in the RUC model microphysics. The CNTL experiment shows an area of 0.12-0.14 g kg in the cold air north of the surface front associated with the heavier precipitation depicted in Fig. S10. The precipitation condensate mixing ratio in the no-profiler experiment is about 20% less. These differences in the three-dimensional flow from assimilating profiler observations appear to be responsible for the improved precipitation forecast in the CNTL experiment. This example of profiler impact in a difficult forecast situation is typical of those cited by NWS operational forecasters in the sidebar in the main article.

c. 8 May 2003 Oklahoma tornado case

Isolated supercell thunderstorms moved through central and northeastern Oklahoma in the late afternoon on 8 May 2003, including a destructive tornado that passed just south of Oklahoma City, resulting in more damage than any Oklahoma tornado since 3 May 1999. Again, RUC parallel cycles were run for a 24-h period with and without wind profiler data, as for the 3 May case. Full hourly VAD data were assimilated in both experiments for this case. Difference (CNTL-EXP) fields (Fig. S15) showed that assimilation of hourly profiler data resulted in a band of increased CAPE (by over 1000 J kg^{-1}) and helicity (by over 75 m^{-2} s^{-2}) in the area of storm initiation in central Oklahoma. Thus, the profiler data again enhanced indicators for severe weather in the area where such storms formed. A similar pattern (not shown) was found for another set of RUC

profiler impact experiments on 4 May 2003, the date of a major multi-state tornado outbreak.

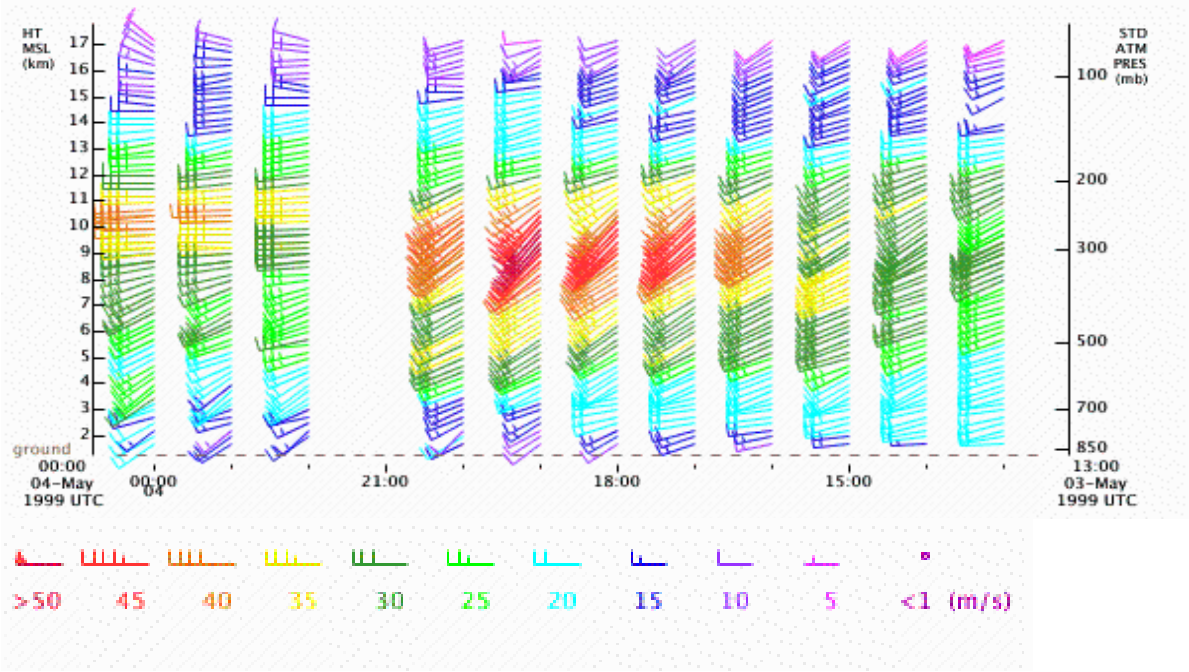

Fig.S1. Tucumcari, New Mexico (TCUM5) profiler time series valid for 1300 UTC 3 May – 0000 UTC 4 May 1999. Wind speed in m s^{-1}, coded by color in legend at bottom.

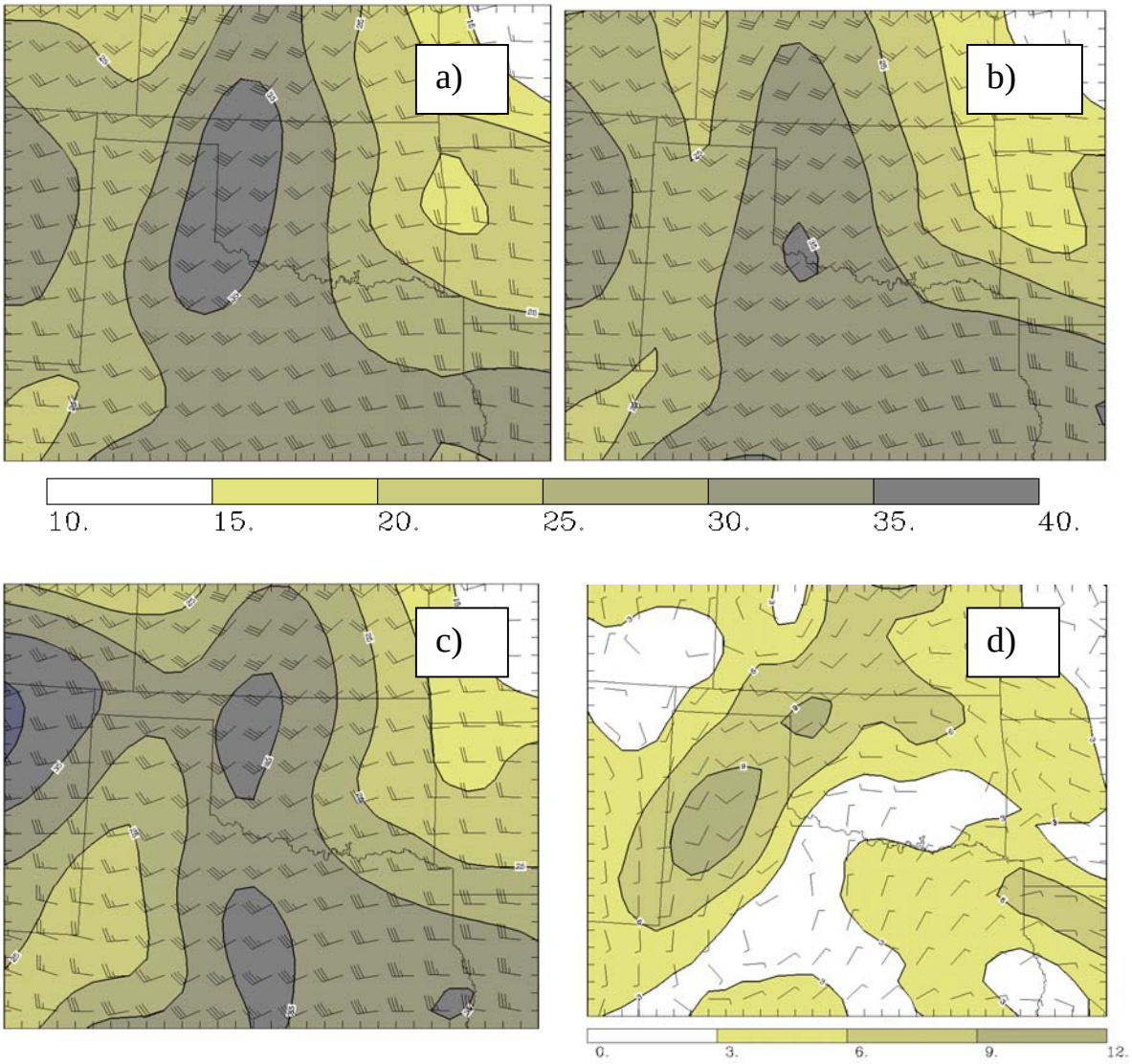

Fig. S2. 6-h forecasts of 300 hPa wind ($m\,s^{-1}$) for a) CNTL (top left) and b) EXP (no profiler,top right) initialized at 1800 UTC 3 May 1999 and valid at 0000 UTC 4 May 1999. c) verifying (CNTL) analysis at 0000 UTC 4 May 1999 (lower left) and d) CNTL-EXP difference between 6-h forecasts (a) – b)).

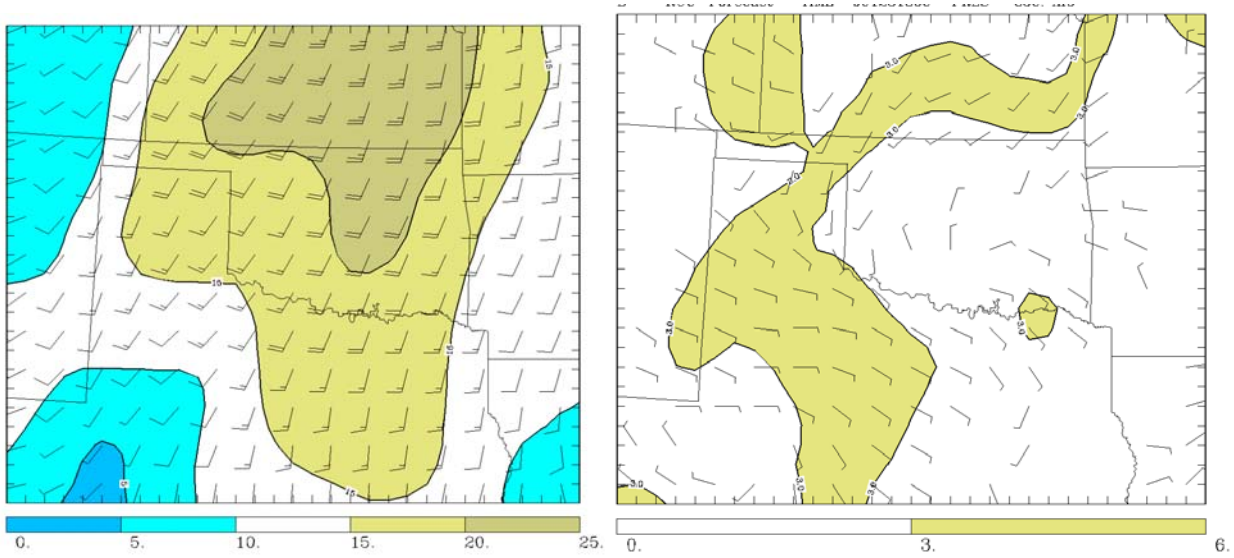

Fig S3. a) 850-hPa (CNTL) wind analysis valid at 0000 UTC 4 May 1999, b) CNTL-EXP difference between 6-h 850-hPa wind forecasts valid at 0000 UTC 4 May 1999.

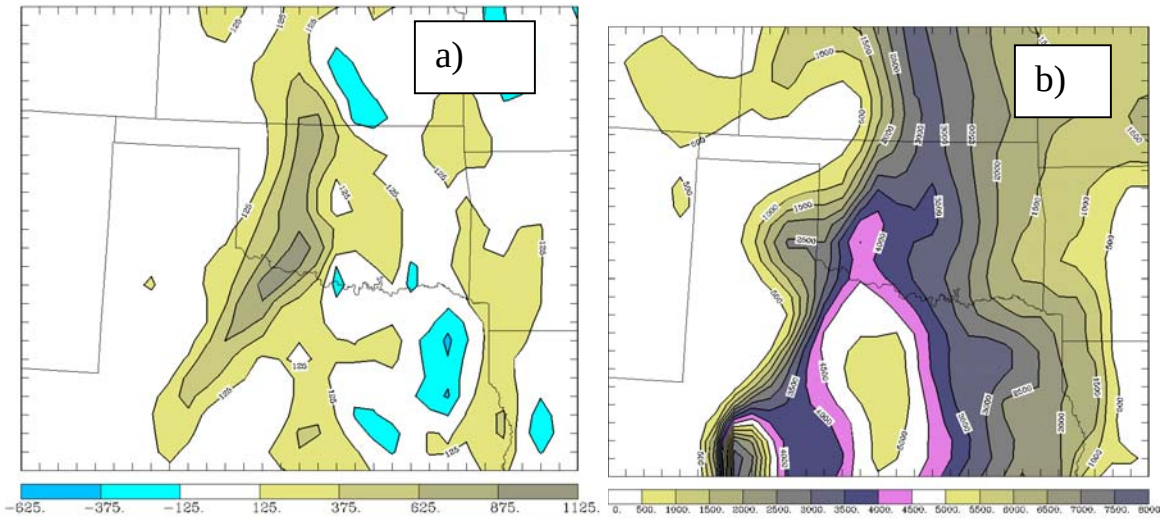

Fig. S4. a) CNTL-EXP difference for 6-h CAPE forecast and b) CAPE values from analysis (CNTL) valid at 2100 UTC 3 May 1999.

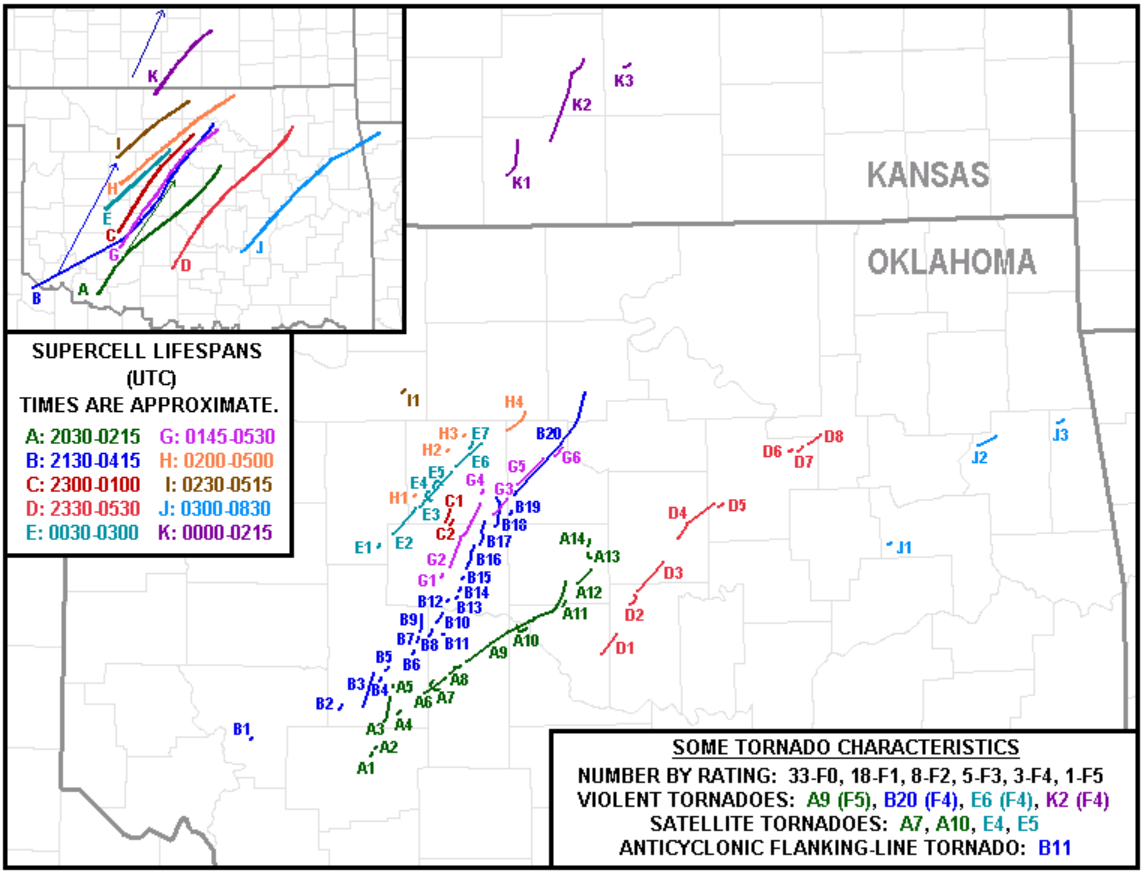

Fig S5. Tornado and supercell (upper left) track summary for 3 May 1999 storms. Provided by NWS Forecast Office, Norman, Oklahoma.

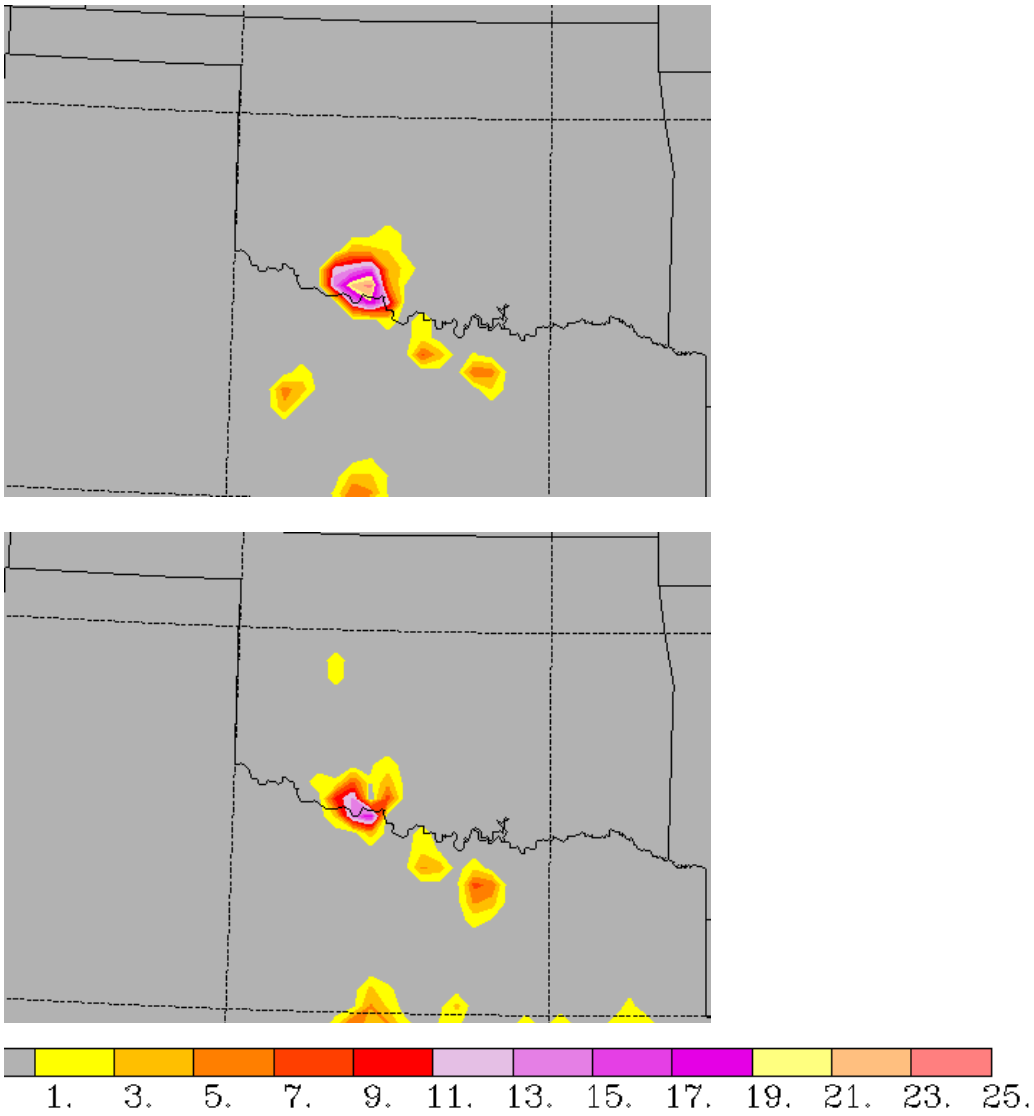

Fig. S6. 6-h predictions of 3-h accumulated precipitation for period 2100 UTC 3 May - 0000 UTC 4 May 1999 from CNTL (left) and no-profiler (right) forecasts initialized at 1800 UTC. Contour interval is 2 mm (0.08 in) starting at 1 mm.

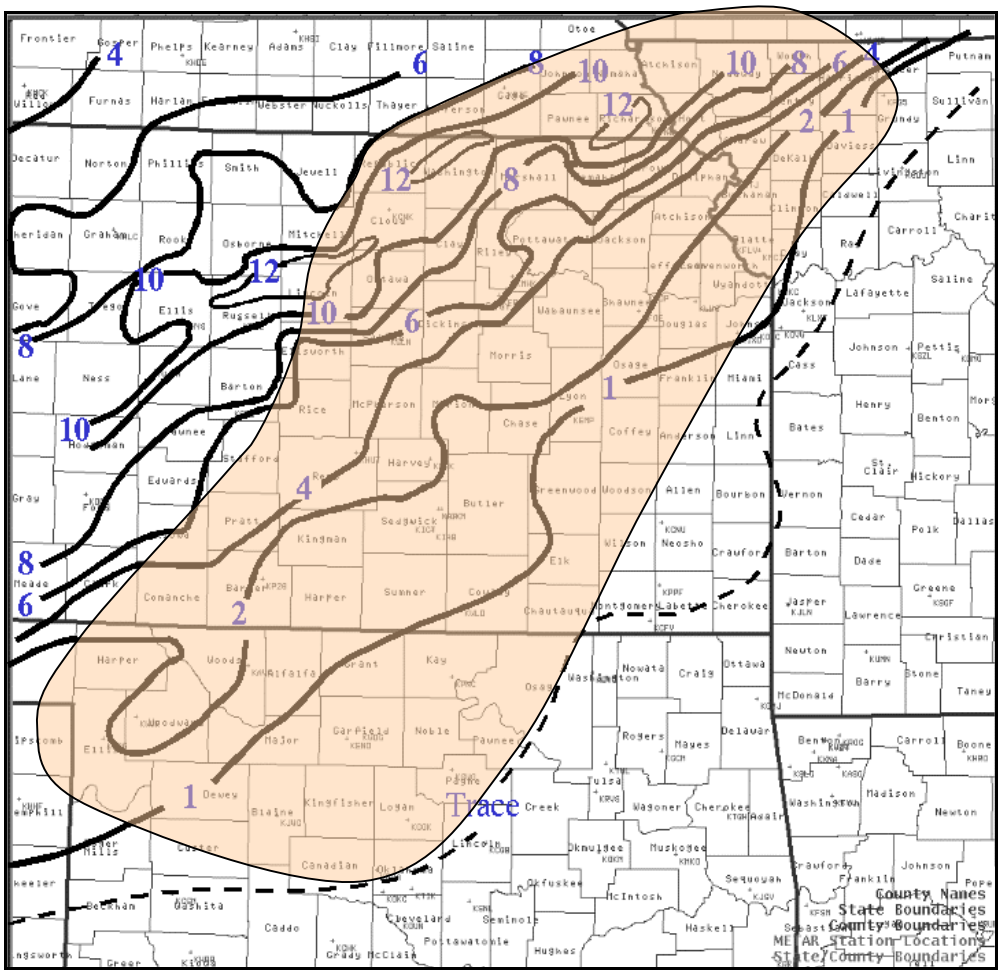

Fig. S7. Snowfall (in) for 24-h period ending at 1200 UTC 9 Feb 2001. Shading indicates areas of sleet or freezing rain accumulation.

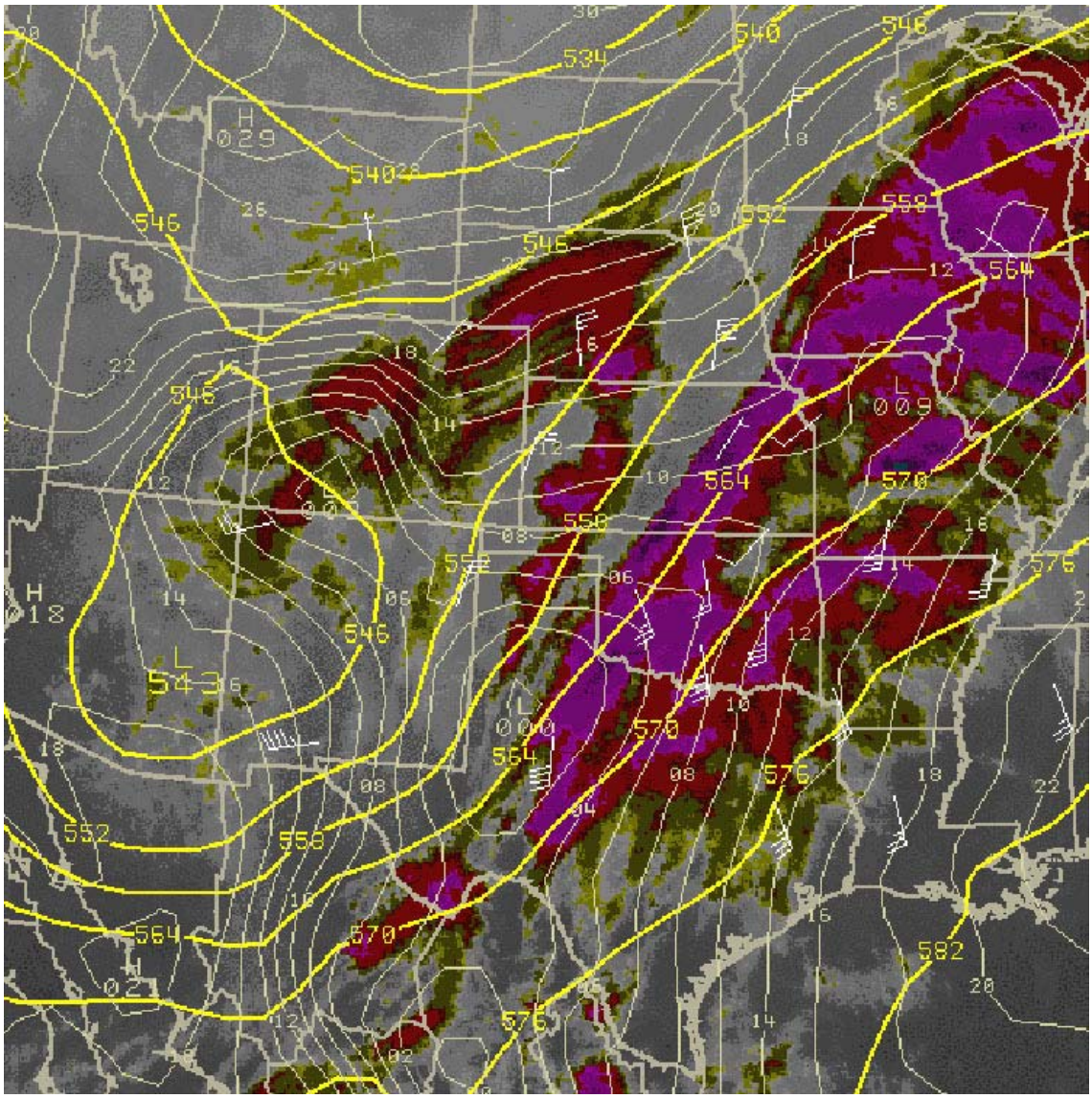

Fig. S8. RUC 500 hPa height (dm) and sea-level pressure (hPa) analyses and 500-m AGL (above ground level) profiler observations with infrared satellite image for 0000 UTC 9 Feb 2001. (From AWIPS).

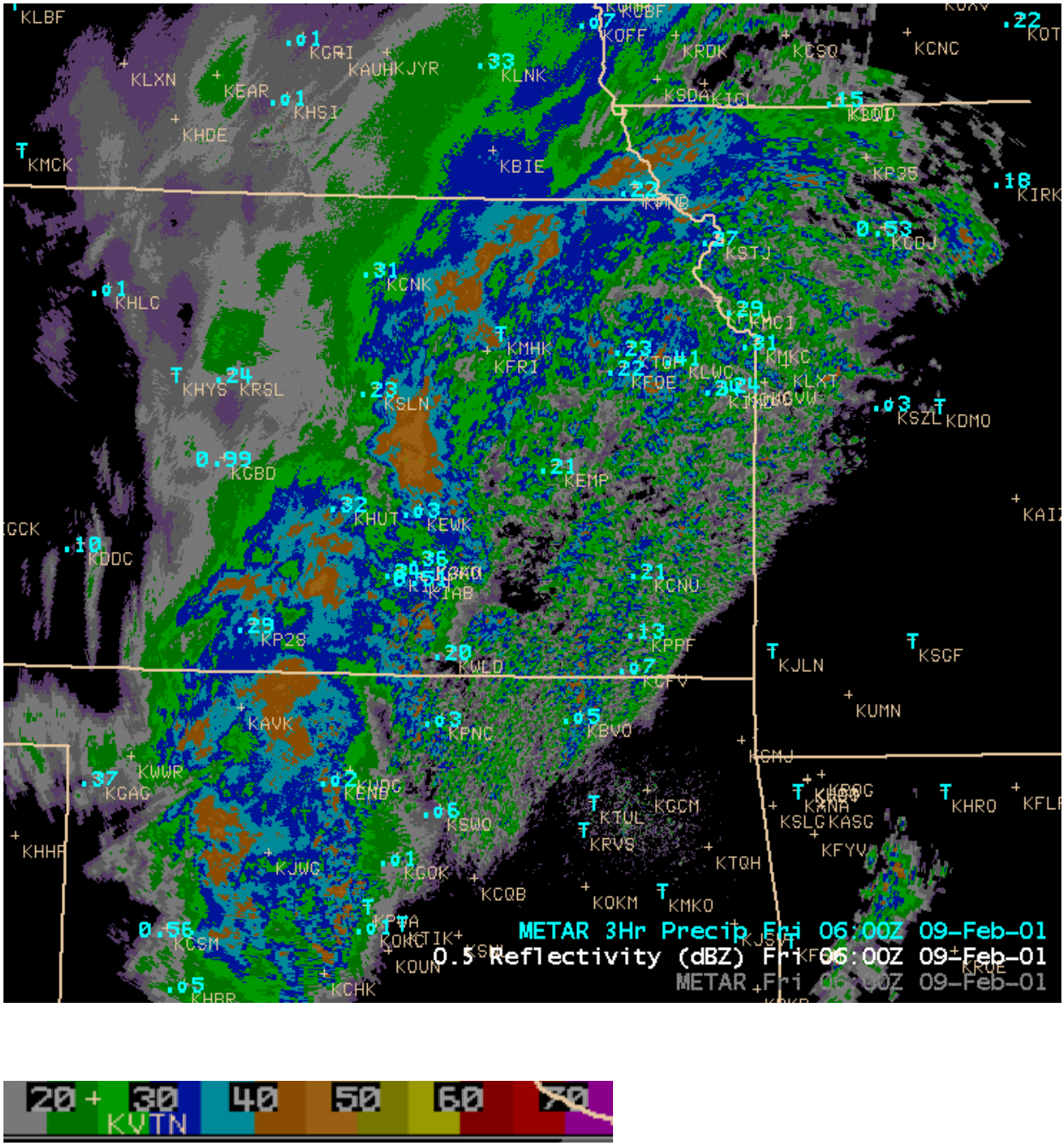

Figure S9. Radar reflectivity (0.5° elevation scan, dBZ color scale shown at bottom) valid at 0600 UTC 9 February 2001 and METAR precipitation (in) totals for 3-h period ending 0600 UTC. (From AWIPS).

Snow

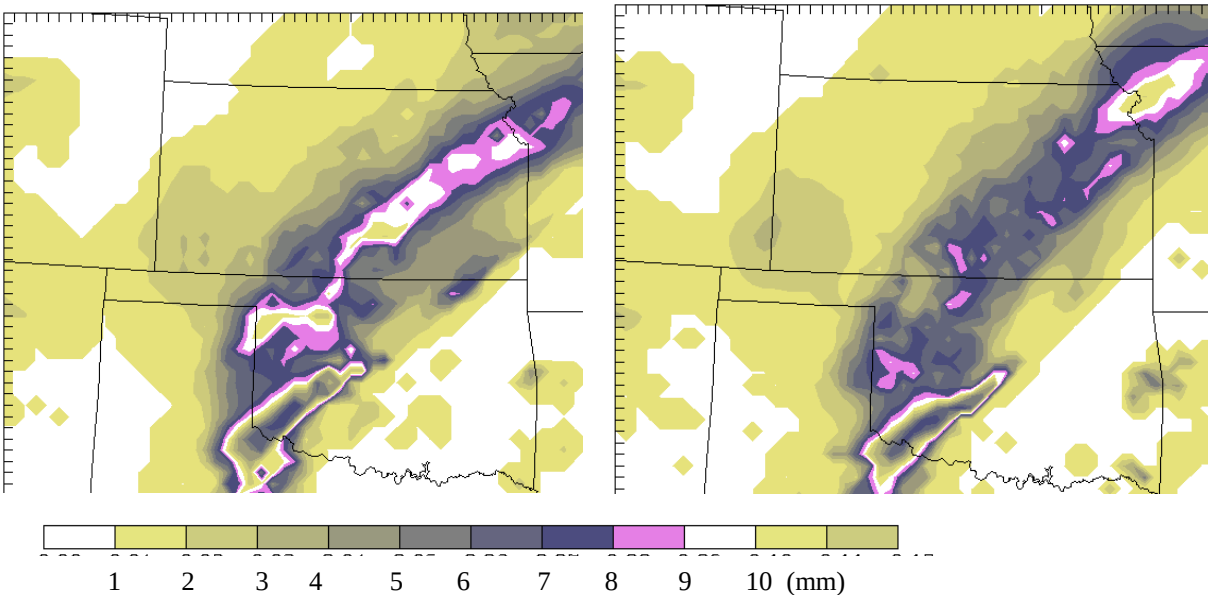

Fig. S10. Forecast 3-h precipitation (mm) for 0300-0600 UTC 9 Feb 2001 from CNTL (left) and no-profiler experiments (right), forecasts initialized at 0300 UTC.

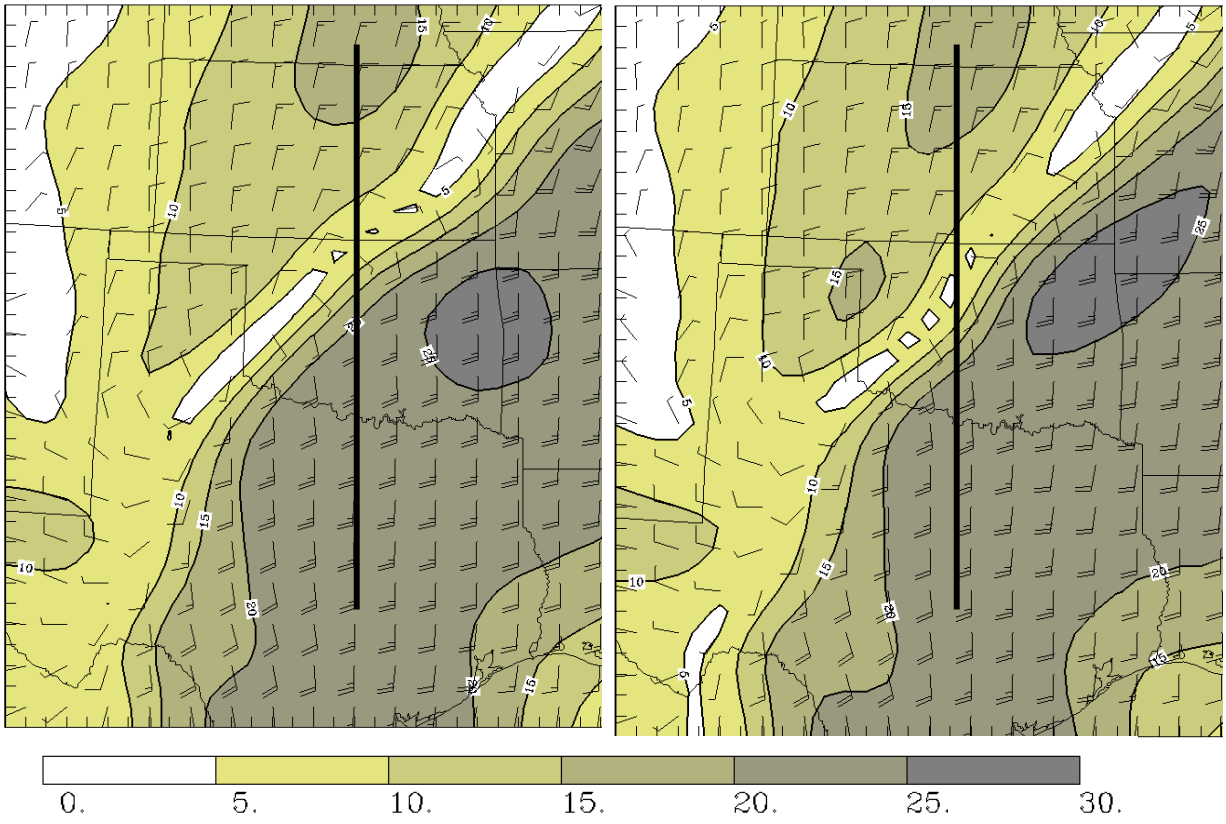

Fig. S11. 900-hPa wind analysis for 0300 UTC 9 February 2001 from CNTL (left) and no-profiler (right) experiments. Contour interval is 5 m s^{-1} with darker shading for higher wind speed and a full barb is 10 m s^{-1}. Solid line is location of cross-section fields displayed in Figs. S12-S14.

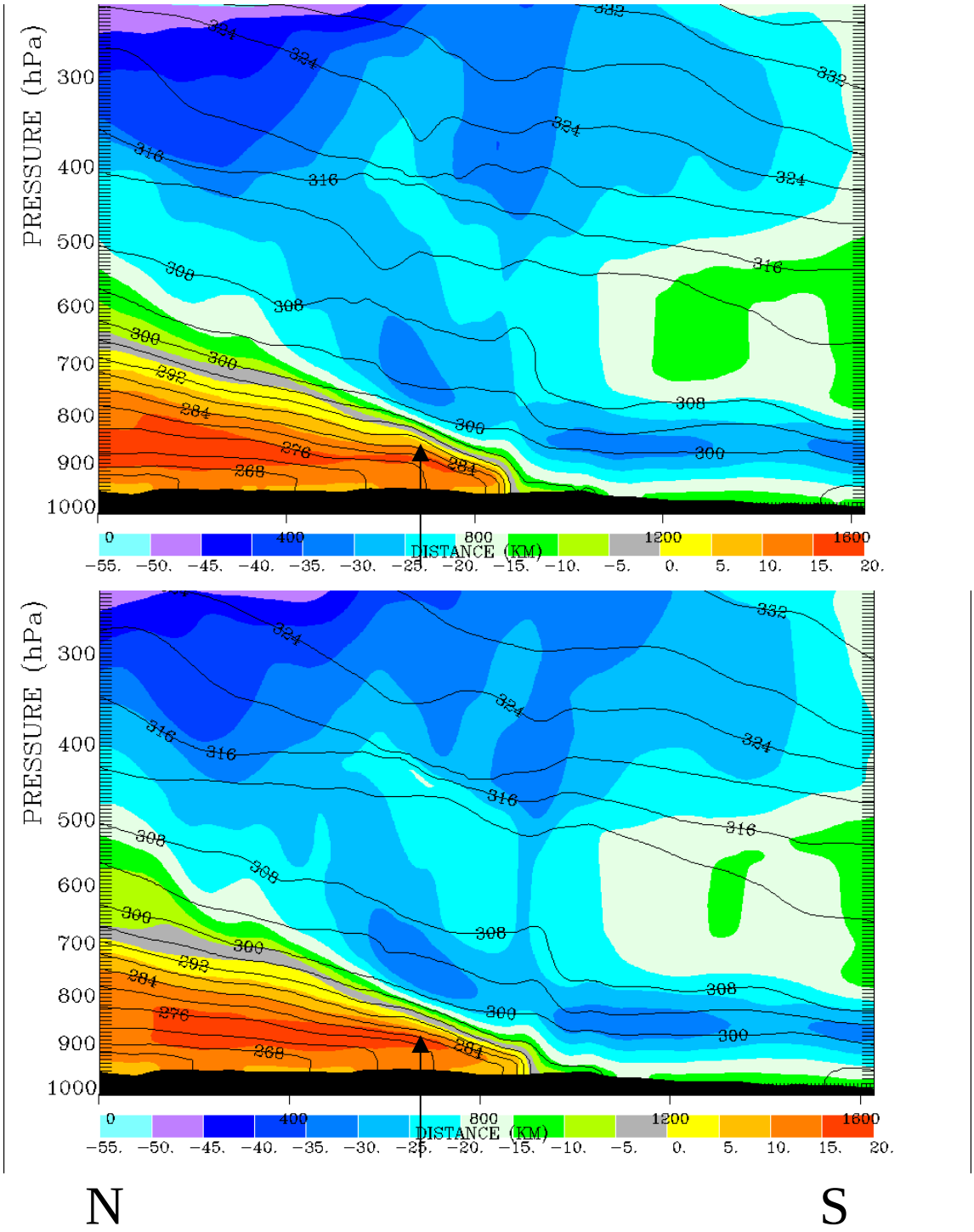

Fig. S12. Vertical cross-section of potential temperature (solid, plotted every 4 K) and along-section wind component (color shading, m s^{-1}, positive – northerly flow, negative – southerly flow) for north-south line shown in Fig. S11 (left end over southern Nebraska and right end over southern Texas). 3-h forecasts valid 0600 UTC 9 February 2001 from CNTL experiment (top) and no-profiler (EXP) experiment (bottom). Position of heavy observed precipitation in southern Kansas at 0600 UTC noted by position of arrow.

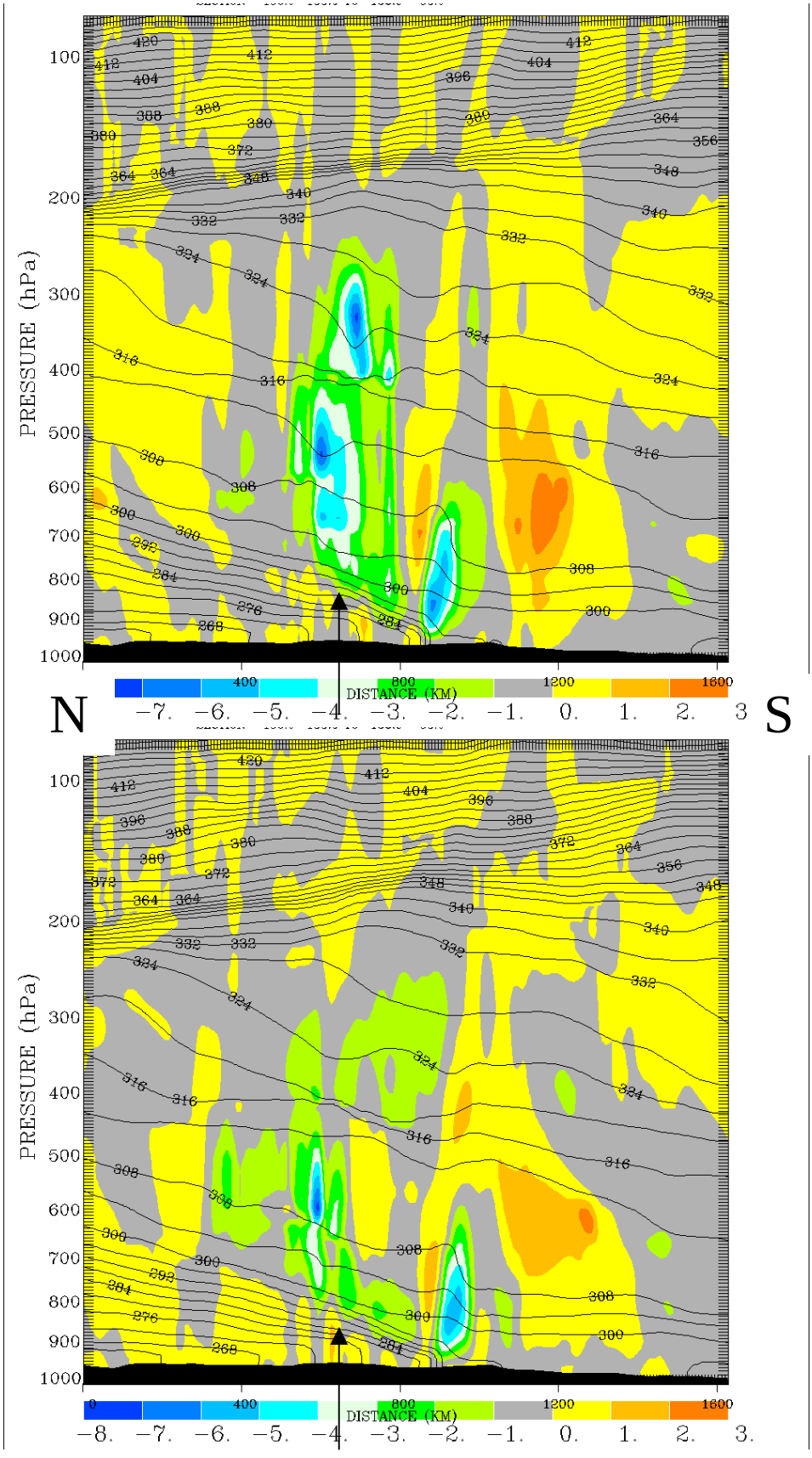
PRESSURE (hPa)
100
200
300
400
500
600
700
800
900
1000
N
S
DISTANCE (KM)
0
400
800
1200
1600
−8. −7. −6. −5. −4. −3. −2. −1. 0. 1. 2. 3.

Fig. S13. Same as Fig. S12 but showing vertical velocity, $\times 10$ μb s^{-1}, e.g., -5 = -50 μb s^{-1} (upward motion).

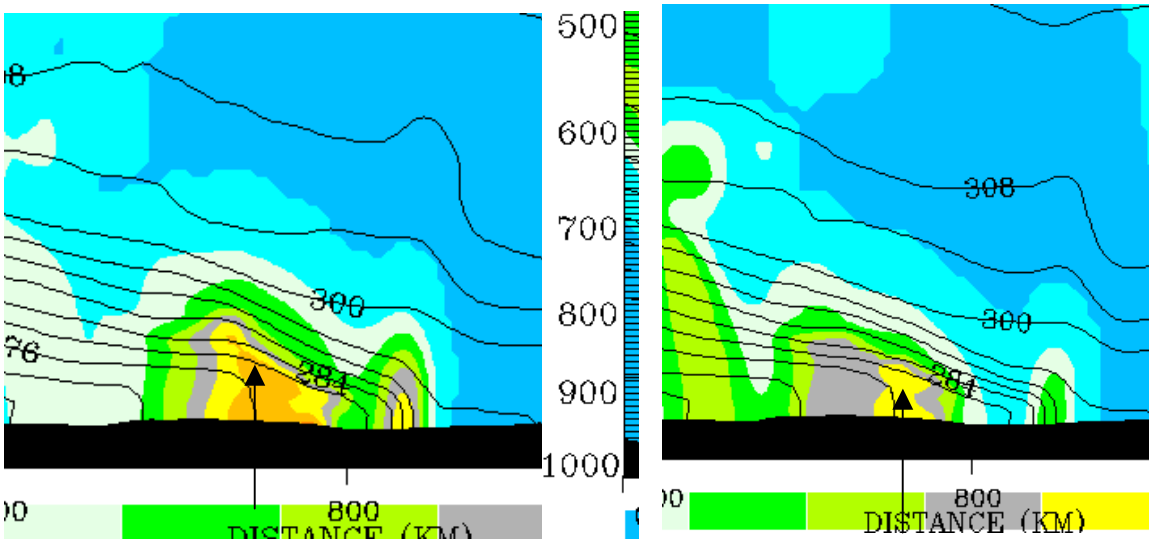

Fig. S14. Same as Fig. S12 but combined precipitation hydrometeor (snow, rain, graupel) mixing ratio (g kg^{-1}) zoomed over center of vertical cross-section shown in Figs. S12 and S13.

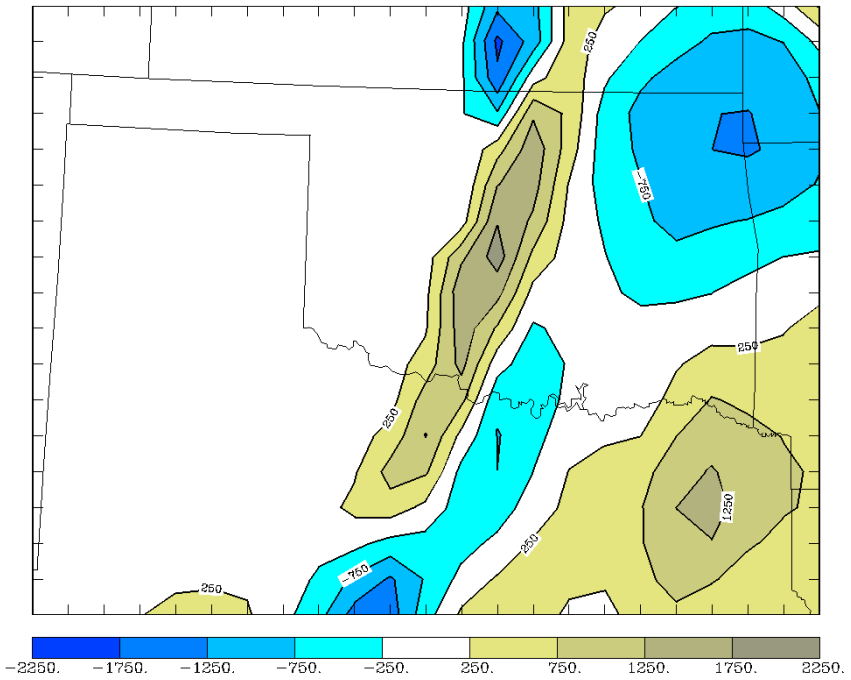

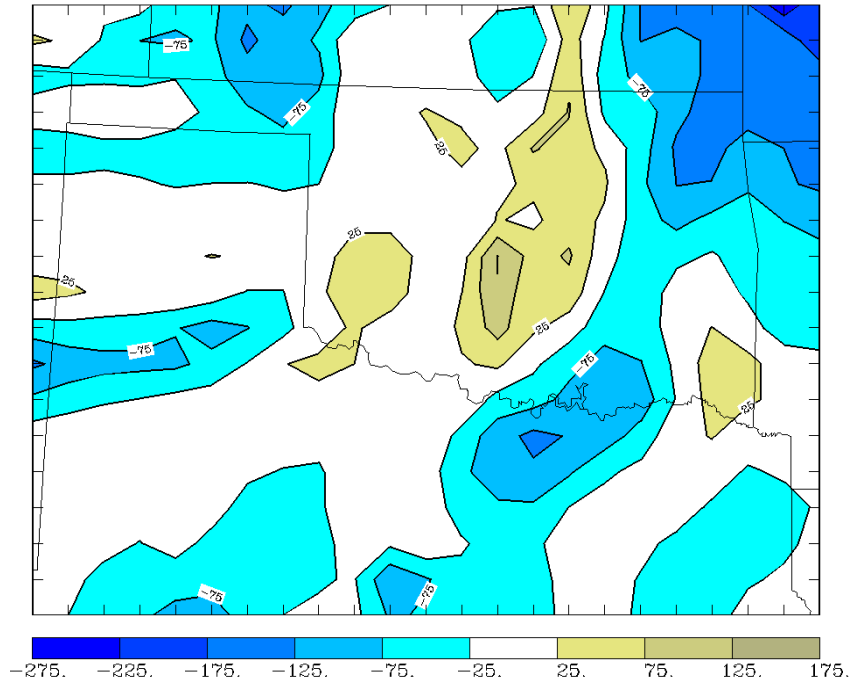

Fig. S15. CAPE and helicity differences from inclusion of wind profiler data for 8 May 2003 case. CNTL-EXP difference for 3-h forecasts initialized at 2100 UTC 8 May 2003. a) CAPE (J kg^{-1}) and b) helicity (m^{-2} s^{-2}).